European Journal of Medicinal Chemistry 217 (2021) 113325

Contents lists available at ScienceDirect

European Journal of Medicinal Chemistry

journal homepage: http://www.elsevier.com/locate/ejmech

Discovery and optimization of novel 3-benzyl-*N*-phenyl-1*H*-pyrazole-5-carboxamides as bifunctional antidiabetic agents stimulating both insulin secretion and glucose uptake

Jeyun Jo [a, †], Dahae Lee [b, †], Yeong Hye Park [a], Hyeonjin Choi [a], Jinhee Han [a], Do Hwi Park [b], You-Kyung Choi [b], Jinsook Kwak [a], Min-Kyu Yang [c], Jin-Wook Yoo [a], Hyung Ryong Moon [a], Dongho Geum [d], Ki Sung Kang [b, *], Hwayoung Yun [a, *]

[a] College of Pharmacy, Pusan National University, Busan, 46241, Republic of Korea
[b] College of Korean Medicine, Gachon University, Seongnam, 13120, Republic of Korea
[c] Mother's Pharmaceutical, Seoul, 08506, Republic of Korea
[d] Department of Biomedical Sciences, Korea University Medical School, Seoul, 02841, Republic of Korea

ARTICLE INFO

Article history:
Received 8 December 2020
Received in revised form
8 February 2021
Accepted 19 February 2021
Available online 6 March 2021

Keywords:
Type 2 diabetes mellitus (T2DM)
3-Benzyl-*N*-phenyl-1*H*-pyrazole-5-carboxamide
Glucose-stimulated insulin secretion (GSIS)
Glucose stimulation index (GSI)
Structure-activity relationship (SAR)

ABSTRACT

A novel series of 3-benzyl-*N*-phenyl-1*H*-pyrazole-5-carboxamides was designed, synthesized and evaluated for their biological activities on glucose-stimulated insulin secretion (GSIS). The cytotoxicity of all 41 novel compounds was screened to assess their pharmacological safety in pancreatic β-cells. A two-step optimization process was carried out to establish the structure-activity relationship for this class and subsequently we identified the most active analogue **26**. Further modification study of **26** evidenced the necessity of *N*-hydrogens in the core architecture. Protein expression analysis suggested that **26** increases insulin secretion via the activation of the upstream effector of pancreatic and duodenal homeobox 1 (PDX-1), which is an important factor promoting GSIS. Moreover, the administration of **26** effectively augmented glucose uptake in C2C12 myotube cells via the suppression of Mitsugumin 53 (MG53), an insulin receptor substrate 1 (IRS-1) ubiquitination E3 ligase.

1. Introduction

Type 2 diabetes mellitus (T2DM), which represents approximately 90% of all cases of diabetes [1], is characterized by persistent hyperglycemia caused by abnormalities in insulin action and β-cell function [2,3]. T2DM affected more than 400 million people worldwide in 2018 and this number is projected to rise to about 500 million by 2030 [4,5]. T2DM causes a series of dysfunctions in multiple organs and tissues and can result in severe chronic complications, such as end-stage renal disease, blindness, arterial disease, slow wound healing, and limb amputation [6]. Numerous therapeutic options for the treatment of T2DM have been developed but only a minority of patients achieve long-term glycaemic control [7,8].

One of the primary factors associated with the development of T2DM is a decrease in glucose-stimulated insulin secretion (GSIS) in pancreatic β-cells [9,10]. Sulfonylureas, which are commonly used oral insulinotropic agents in the clinical management of T2DM [11], increase insulin secretion from β-cells by closing K-ATP channels in the cell membrane. However, drugs in this class often elicit hypoglycemia because they continuously stimulate insulin secretion independently of blood glucose level [11]. In order to compensate for the major drawback of sulfonylureas, glucose-dependent insulin secretagogues, including dipeptidyl peptidase-4 (DPP-4) inhibitors and ligands that target islet G-protein-coupled receptors (GPCRs), have recently been developed [12]. Nonetheless, recent studies have suggested that DPP-4 inhibitors cause severe joint pain and glucagon-like peptide-1 (GLP-1) receptor agonists increase the risk of cholelithiasis [13,14]. Moreover, these agents may be associated with an increased risk of cholangiocarcinoma [15]. Continuous efforts for the development of improved therapies, such as G-protein-coupled receptor (GPR) 40 and GPR119 agonists, are ongoing to address the limitations of current treatments; however, these

* Corresponding authors.
E-mail addresses: kkang@gachon.ac.kr (K.S. Kang), hyun@pusan.ac.kr (H. Yun).
† These authors contributed equally to this work.

https://doi.org/10.1016/j.ejmech.2021.113325
0223-5234/

options are still not clinically available [16,17]. The identification of novel molecules and pathways that have the potential to correct glycaemia via the stimulation of GSIS is, therefore, highly desirable.

In an effort to discover novel antidiabetic agents, an in-house chemical library containing approximately heterocycle-based 500 compounds was screened using INS-1 cells with a GSIS assay. The INS-1 cell line has been widely used for studies of glucose-dependent β-cell function because it secretes insulin in response to concentrations of glucose within the physiological range [18]. From the preliminary screening, we identified hit compound **1** which exhibited a strong insulin secretion activity, equal to that of a representative sulfonylurea gliclazide, at a concentration of 10 μM (Fig. 1A). Interestingly, compound **1** consists of a core 5-carboxamidopyrazole and two *para*-halo-substituted benzene rings and has relatively good lead-like properties (MW $\leq$ 460, rings $\leq$ 4, hydrogen-bond donors $\leq$ 5, hydrogen-bond acceptors $\leq$ 9, and $-4 \leq$ LogP $\leq$ 4.2) [19]. Herein, we designed and synthesized a new set of 3-benzyl-*N*-phenyl-1*H*-pyrazole-5-carboxamides by decorating various substituents on both benzene rings (Fig. 1B). Furthermore, we attempted to optimize our analogues in detail and establish a brief structure-activity relationship (SAR).

2. Results and discussion

2.1. Chemistry

Based on the structure of hit **1**, we initially decided to introduce various substituents on the para positions of both benzene rings. The synthetic route for the final analogues **1** and **6**–**22** is illustrated in Scheme 1. The commercially available phenylacetones **2a**–**c** were first condensed with diethyl oxalate in the presence of *t*-BuOK, followed by a second condensation of the resulting 2,4-dioxopentanoates **3a**–**c** with hydrazine under acidic conditions to afford the desired pyrazoles **4a**–**c**. The key intermediates **5a**–**c** were smoothly produced by the simple saponification of the corresponding pyrazoles **4a**–**c**. Finally, 1-ethyl-3-(3-dimethylaminopropyl)carbodiimide (EDC) coupling of **5a**–**c** with various anilines provided 3-benzyl-*N*-phenyl-1*H*-pyrazole-5-carboxamides **1** and **6**–**22**.

We subsequently turned our attention to the derivatization of the potent analogue **9** to find out the anti-diabetic effect of the methoxy group. With the previously prepared building blocks **5a**–**c** in hand, we manipulated similar EDC couplings with diversely methoxy-substituted anilines (Scheme 2). The new 3-benzyl-*N*-phenyl-1*H*-pyrazole-5-carboxamides **23**–**40** were efficiently obtained.

Lastly, we then executed further optimization of the best analogue **26**, which possessing a 2,4-dimethoxy group, to confirm SAR analysis. A similar attempt utilizing the 4-step process depicted in Scheme 1 successfully resulted in the final 3-benzyl-*N*-phenyl-1*H*-pyrazole-5-carboxamides, **41** (R^1 = 3-Cl) and **42** (R^1 = 2-Cl), starting from the commercially available phenylacetones **2d** and **2e**, respectively (Scheme 3A). The exposure of the building block **5a** to oxalyl chloride and the coupling of the resulting acid chloride with 2,4-dimethoxy-*N*-methylaniline smoothly yielded 3-benzyl-*N*-methyl-*N*-phenyl-1*H*-pyrazole-5-carboxamide **43** (Scheme 3B). As a final entry in our diversification, the common intermediate **4a** was subjected to *N*-alkylation with iodomethane and benzylic oxidation with *t*-butyl hydroperoxide (TBHP) [20] to afford *N*-methylpyrazole ester **44** and 4-chlorobenzoylpyrazole ester **47**, respectively (Scheme 3C). Finally, the saponification of esters **44** and **47**, followed by the amidation of the resulting carboxylic acids **45** and **48**, furnished 3-benzyl-*N*-phenyl-1*H*-pyrazole-5-carboxamides **46** and **49**, respectively.

2.2. Biological evaluation

2.2.1. GSIS assay

The synthesized compounds were evaluated for their insulin releasing activities in INS-1 cells by measuring glucose-stimulated insulin secretion (GSIS). The GSIS data can be normalized as a glucose stimulation index (GSI), which is calculated as the ratio of the insulin value under high-glucose divided by that under low-glucose conditions [21]. INS-1 cells were exposed to 10 μM of the compounds for 2 h and stimulated with 3.3 mM and 16.7 mM glucose for 1 h. Gliclazide was run in parallel as a positive control drug. Additionally, the viability of INS-1 cells was determined after

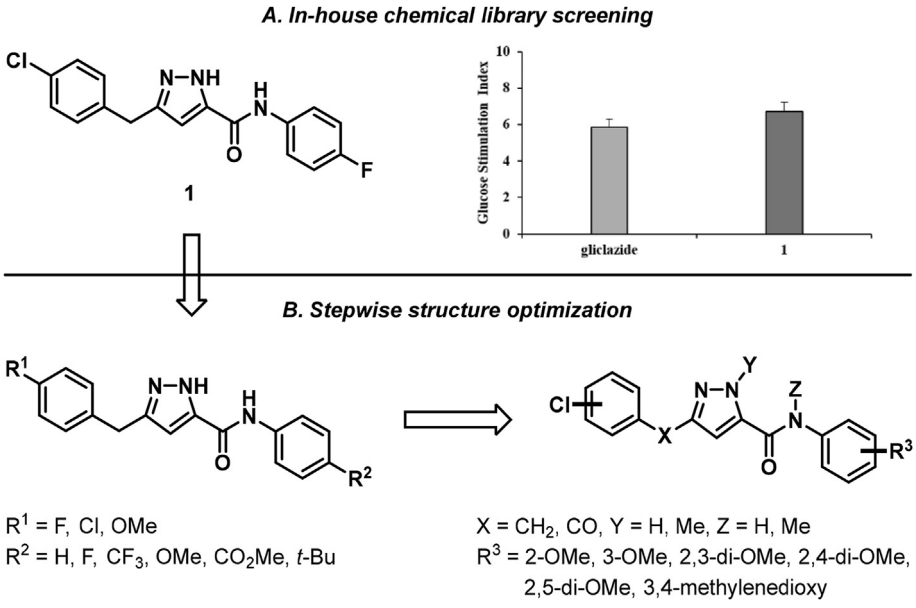

Fig. 1. (A) Identification of hit compound **1**; (B) Optimization of novel 3-benzyl-*N*-phenyl-1*H*-pyrazole-5-carboxamides.

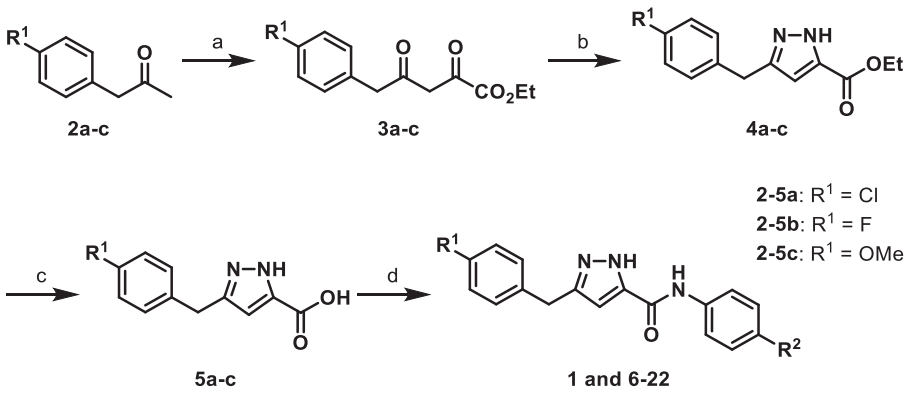

1: R^1 = Cl, R^2 = F
6: R^1 = Cl, R^2 = H
7: R^1 = Cl, R^2 = *t*-Bu
8: R^1 = Cl, R^2 = CF_3
9: R^1 = Cl, R^2 = OMe
10: R^1 = Cl, R^2 = CO_2Me
11: R^1 = F, R^2 = F
12: R^1 = F, R^2 = H
13: R^1 = F, R^2 = *t*-Bu
14: R^1 = F, R^2 = CF_3
15: R^1 = F, R^2 = OMe
16: R^1 = F, R^2 = CO_2Me
17: R^1 = OMe, R^2 = F
18: R^1 = OMe, R^2 = H
19: R^1 = OMe, R^2 = *t*-Bu
20: R^1 = OMe, R^2 = CF_3
21: R^1 = OMe, R^2 = OMe
22: R^1 = OMe, R^2 = CO_2Me

Scheme 1. Synthesis of 3-benzyl-*N*-phenyl-1*H*-pyrazole-5-carboxamides **1** and **6**–**22**. Reagents and conditions: (a) $(CO_2Et)_2$, *t*-BuOK, toluene, 0 °C, 67–97%; (b) $H_2NNH_2{\cdot}H_2O$, AcOH, 67–93%; (c) $LiOH{\cdot}H_2O$, THF/H_2O (2:1), 50 °C, 71–89%; (d) R^2-C_6H_4-NH_2, EDC·HCl, DMAP, CH_2Cl_2, 18–79%.

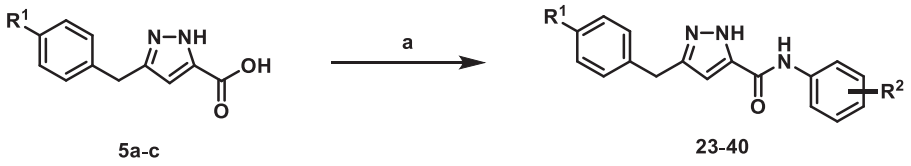

23: R^1 = Cl, R^2 = 2-OMe
24: R^1 = Cl, R^2 = 3-OMe
25: R^1 = Cl, R^2 = 2,3-di-OMe
26: R^1 = Cl, R^2 = 2,4-di-OMe
27: R^1 = Cl, R^2 = 2,5-di-OMe
28: R^1 = Cl, R^2 = 3,4-methylenedioxy
29: R^1 = F, R^2 = 2-OMe
30: R^1 = F, R^2 = 3-OMe
31: R^1 = F, R^2 = 2,3-di-OMe
32: R^1 = F, R^2 = 2,4-di-OMe
33: R^1 = F, R^2 = 2,5-di-OMe
34: R^1 = F, R^2 = 3,4-methylenedioxy
35: R^1 = OMe, R^2 = 2-OMe
36: R^1 = OMe, R^2 = 3-OMe
37: R^1 = OMe, R^2 = 2,3-di-OMe
38: R^1 = OMe, R^2 = 2,4-di-OMe
39: R^1 = OMe, R^2 = 2,5-di-OMe
40: R^1 = OMe, R^2 = 3,4-methylenedioxy

Scheme 2. Synthesis of 3-benzyl-*N*-phenyl-1*H*-pyrazole-5-carboxamides **23**–**40**. Reagents and conditions: (a) R^2-C_6H_4-NH_2 or R^2-C_6H_3-NH_2, EDC·HCl, DMAP, CH_2Cl_2, 8–58%.

treatment with newly synthesized compounds using the 3-(4,5-dimethythiazol-2-yl)-2,5-diphenyltetrazolium bromide (MTT) assay.

The GSI value and cytotoxicity of the initially designed derivatives **6**–**22** at a concentration of 10 μM are summarized in Table 1. Our efforts were focused on exploring the best substituents on both benzene rings of hit compound **1**. Generally, the 4-chlorobenzene (**6**–**10**) series at the part A position displayed improved GSI values compared with the 4-fluorobenzene (**11**–**16**) and 4-methoxybenzene (**17**–**22**) series. Among the 4-chlorobenzylpyrazoles (**6**–**10**), compound **9**, which containing a 4-methoxy group at the part B position, exhibited the best insulin-secreting activity, which was more potent than that of hit **1**. The removal of the 4-fluoro substituent of **1** resulted in a slightly lower potency (compound **6**). A similar behavior was observed with the replacement of the fluoro group of **1** with a *tert*-butyl group (compound **7**). However, compounds **8** and **10**, which possess a 4-CF_3 and a 4-CO_2Me at part B, respectively, did not lead to any improvement in insulin secretion under high-glucose conditions. Taken together, the GSI value of the first designed series suggests that the presence of an electron-donating group at part B would be beneficial for insulin-secreting activity. Gratifyingly, none of synthesized compounds exhibited significant cytotoxicity against INS-1 cells at the treated concentrations.

At the stage of further optimization, 18 new analogues (**23**–**40**), which were structurally derived from compound **9**, were tested for GSIS at a concentration of 5 μM (Table 2). Generally, the 4-chlorobenzene (**23**–**28**) and 4-fluorobenzene (**29**–**34**) series at the part A position seemed to be more effective than the 4-methoxybenzene (**35**–**40**) series. Among them, compounds **26**, **27**, **29**, and **30** were found to be more potent than compound **9** at the treated concentration. Especially, 4-chlorobenzene analogue

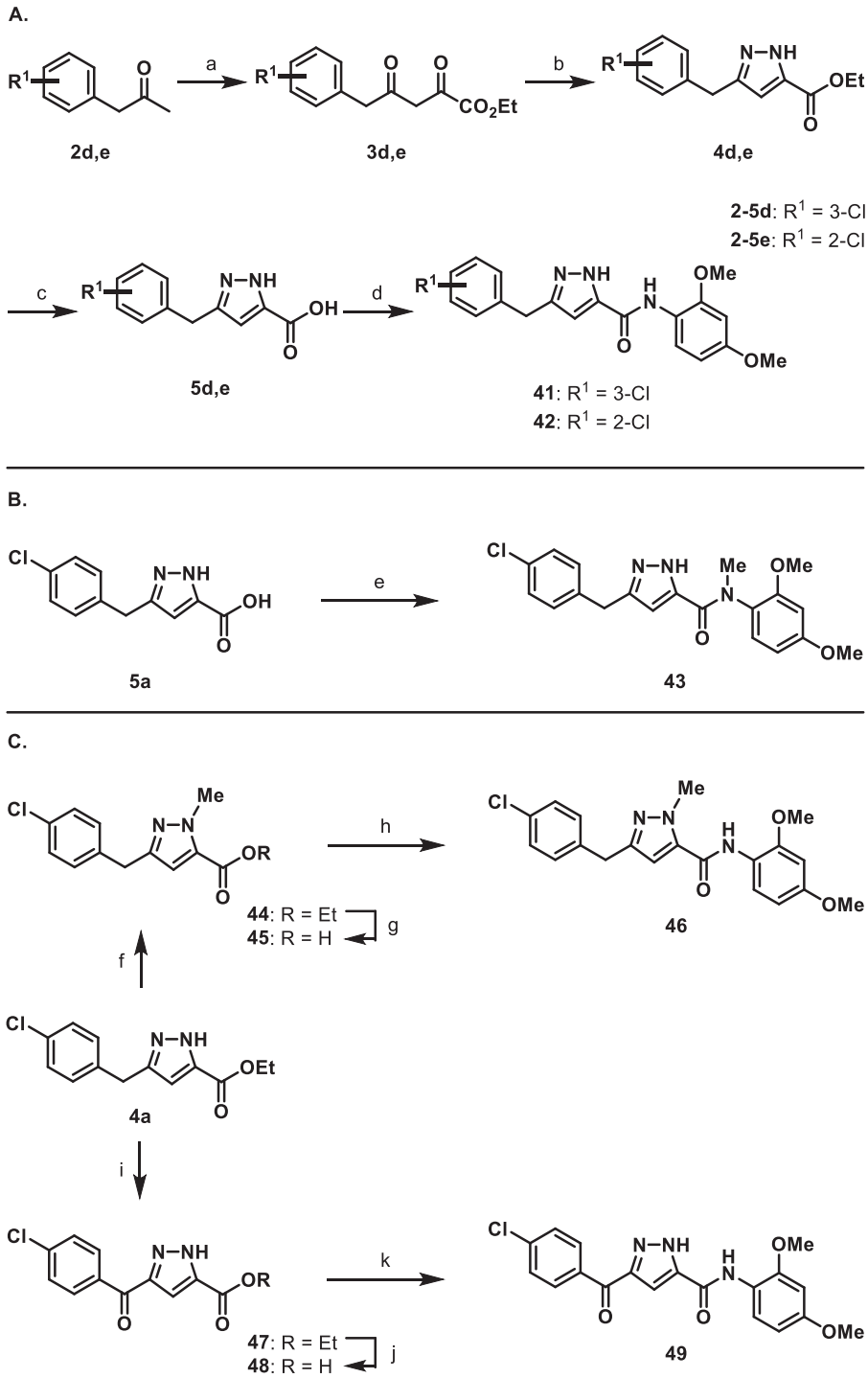

Scheme 3. Synthesis of 3-benzyl-*N*-phenyl-1*H*-pyrazole-5-carboxamides **41**–**43**, **46**, and **49**. Reagents and conditions: (a) $(CO_2Et)_2$, *t*-BuOK, toluene, 0 °C, 68–77%; (b) $H_2NNH_2 \cdot H_2O$, AcOH, 69–79%; (c) $LiOH \cdot H_2O$, THF/H_2O (2:1), 50 °C, 71–95%; (d) 2,4-dimethoxyaniline, EDC·HCl, DMAP, CH_2Cl_2, 60–93%; (e) 2,4-dimethoxy-*N*-methylaniline, $(COCl)_2$, Et_3N, DMF, CH_2Cl_2, 54%; (f) MeI, K_2CO_3, DMF, 44%; (g) $LiOH \cdot H_2O$, THF/H_2O (2:1), 50 °C, 95%; (h) 2,4-dimethoxyaniline, $(COCl)_2$, Et_3N, DMF, CH_2Cl_2, 87%; (i) TBHP, 120 °C, 96%; (j) $LiOH \cdot H_2O$, THF/H_2O (2:1), 50 °C, 92%; (k) 2,4-dimethoxyaniline, EDC·HCl, HOBt·H_2O, DMAP, DIPEA, DMF, 81%.

26, which containing a 2,4-dimethoxy group at the part B position, showed the highest insulin-secreting activity, with a GSI value of 14.9, which was approximately six-fold higher than that of **9**. Likewise, 4-fluorobenzene analogue **30**, which possessing a 3-methoxy group at the part B position, also exhibited substantial insulin-secreting activity. These results suggest that the potential targets of the 4-chlorobenzene and 4-fluorobenzene series might be different or do not share the same binding mode. The introduction of a methoxy group to the part A benzene and a methylenedioxy group to the part B benzene were not helpful to enhance potency. Furthermore, all compounds **23**–**40** had no cytotoxic effects on INS-1 cells at a concentration of 10 μM (Table 2).

These results encouraged us to extend the SAR study by exploring an additional modification of the best analogue **26**. As

Table 1
GSIS activity and cytotoxicity of analogues **6**–**22** on INS-1 cell line.

Comp	GSI[a] at 10 μM	Cell viability at 10 μM (% of untreated control)[b]
1	6.73 ± 0.50	94.9 ± 5.2
6	5.24 ± 2.14	109 ± 2.1
7	4.89 ± 0.04	97.5 ± 4.1
8	1.69 ± 0.12	102 ± 5.3
9	7.59 ± 0.15	101 ± 4.8
10	1.48 ± 0.10	101 ± 3.3
11	1.86 ± 0.08	100 ± 4.0
12	2.00 ± 0.01	100 ± 2.7
13	1.96 ± 0.16	98.6 ± 2.3
14	2.02 ± 0.01	92.8 ± 2.9
15	2.03 ± 0.31	95.6 ± 3.6
16	1.42 ± 0.09	102 ± 3.3
17	2.49 ± 0.19	105 ± 0.4
18	4.40 ± 0.08	105 ± 1.2
19	1.64 ± 0.05	99.4 ± 4.3
20	2.07 ± 0.11	98.4 ± 1.0
21	1.66 ± 0.05	105 ± 0.5
22	1.85 ± 0.01	99.2 ± 2.2
Gliclazide	5.86 ± 0.46	98.7 ± 2.6

[a] Insulin content in 16.7 mM glucose media/insulin content in 3.3 mM glucose media.
[b] Values are the mean ± standard deviation.

Table 2
GSIS activity and cytotoxicity of analogues **9** and **23**–**40** on INS-1 cell line.

Comp	GSI[a] at 5 μM	Cell viability at 10 μM (% of untreated control)[b]
9	2.60 ± 0.07	101 ± 4.8
23	1.56 ± 0.11	98.1 ± 2.3
24	1.54 ± 0.04	96.5 ± 2.1
25	1.85 ± 0.01	98.8 ± 3.5
26	14.9 ± 0.20	96.3 ± 5.5
27	3.25 ± 0.08	97.9 ± 0.8
28	1.29 ± 0.06	101 ± 4.3
29	3.67 ± 0.05	104 ± 0.6
30	7.49 ± 0.63	101 ± 0.7
31	1.16 ± 0.01	102 ± 2.7
32	1.93 ± 0.33	99.9 ± 2.0
33	1.52 ± 0.29	104 ± 1.1
34	1.25 ± 0.003	97.6 ± 1.7
35	1.66 ± 0.03	101 ± 3.2
36	1.55 ± 0.01	102 ± 1.1
37	1.13 ± 0.02	98.9 ± 3.3
38	1.58 ± 0.02	101 ± 2.8
39	2.35 ± 0.15	100 ± 0.3
40	1.13 ± 0.003	102 ± 3.6

[a] Insulin content in 16.7 mM glucose media/insulin content in 3.3 mM glucose media.
[b] Values are the mean ± standard deviation.

Table 3
GSIS activity and cytotoxicity of analogues **41**–**43, 46**, and **49** on INS-1 cell line.

Comp	GSI[a] at 5 μM	Cell viability at 10 μM (% of untreated control)[b]
41	1.29 ± 0.04	97.7 ± 1.9
42	2.43 ± 0.03	102 ± 1.6
43	1.33 ± 0.01	93.3 ± 1.1
46	1.37 ± 0.06	96.2 ± 3.6
49	1.49 ± 0.08	100 ± 2.7
Gliclazide	4.22 ± 0.01	98.7 ± 2.6

[a] Insulin content in 16.7 mM glucose media/insulin content in 3.3 mM glucose media.
[b] Values are the mean ± standard deviation.

depicted in Scheme 3, the parent compound **26** was structurally transformed into 3-chlorobenzene (**41**), 2-chlorobenzene (**42**), *N*-methylamide (**43**), *N*-methylpyrazole (**46**), and 4-chlorobenzoylpyrazole (**49**). These compounds were then subjected to GSIS and MTT assays with gliclazide as a positive control (Table 3). Most novel derivatives exhibited slightly less potent activity (GSI = 1.29–2.43) than gliclazide. Taken together, the 4-chloro substituent in the part A benzene was preferred to other substituents for anti-diabetic activity. The introduction of a methyl group to the amide backbone or the pyrazole ring resulted in the loss of activity, which presumably indicates that both *N*-hydrogen moieties play a crucial role in the insulin-secreting activity of the compounds. Additionally, the insertion of a carbonyl group to the benzylic position, which may have provided a conformationally restricted environment, resulted in low activity. Based on the brief SAR of the 41 derivatives, the most potent analogue **26** was finally selected for detailed biological evaluation. We tested cytotoxicity of compound **26** on two different normal cell lines, LX-2 human hepatic stellate cells and 3T3L-1 mouse embryonic fibroblast cells for further biological evaluation and **26** did not show any toxicity at all the tested concentrations (Fig. S1 in Supplementary Data).

2.2.2. Effect of **26** on protein expression related to pancreatic β-cell function

To gain insight into the potential mechanism of **26** on insulin secretion, we investigated the effects of **26** on protein expression related to pancreatic β-cell function using western blotting (Fig. 2). The activation of serine/threonine kinase Akt, a downstream effector of phosphoinositide 3-kinase (PI3K), is mainly involved in pancreatic β-cell metabolism and survival and the promotion of insulin secretion [22–25]. Previous studies have reported that PI3K/Akt signaling can be activated using a direct binding ligand for PI3K or by the regulation of upstream components such as insulin receptor substrate 2 (IRS-2) [23–26]. Therefore, we first decided to analyze the cellular levels of IRS-2, p-IRS-2, PI3K, p-PI3K, Akt, and p-Akt. As demonstrated in Fig. 2A–D, compound **26** dose-dependently upregulated the expression of p-Akt, p-PI3K, and p-IRS-2 in INS-1 cells, which suggests that IRS-2 is the upstream regulator of PI3K-dependent Akt phosphorylation (Ser473) in response to treatment with **26**. In the additional western blot experiment, we could observe that the expression of peroxisome proliferator-activated receptor-γ (PPAR-γ) and pancreatic and duodenal homeobox 1 (PDX-1) was significantly increased when compound **26** was administered (Fig. 2A, E, and 2F). PDX-1 is an important regulator of glucose-stimulated insulin gene expression and can be transcriptionally regulated by PPAR-γ in INS-1 cells [27,28]. Considering that the PI3K/Akt pathway is critical for the expression and activation of PDX-1 [27,29,30], compound **26** plausibly enhances GSIS by regulating PDX-1 function via the activation of PPAR-γ and IRS-2-mediated PI3K/Akt signaling in pancreatic β-cells [31].

2.2.3. Effect of **26** on glucose uptake in C2C12 myotube cells

As compound **26** showed an ability to activate insulin receptor substrate-associated PI3K activity and Akt phosphorylation, we next examined whether the compound regulates glucose homeostasis in the C2C12 myotube cell line (Fig. 3). Recent studies have suggested that compounds with antidiabetic potential, including several natural products and AMP-activated protein kinase (AMPK) activators, that promote insulin secretion in β-cells via PI3K activation, could dually increase glucose uptake in skeletal muscles [32–37]. Therefore, compound **26** was first evaluated for its capacity to augment glucose uptake in the myotube cell line. With the treatment of **26**, glucose uptake was dose-dependently increased in the absence of insulin (Fig. 3A). To explore the molecular

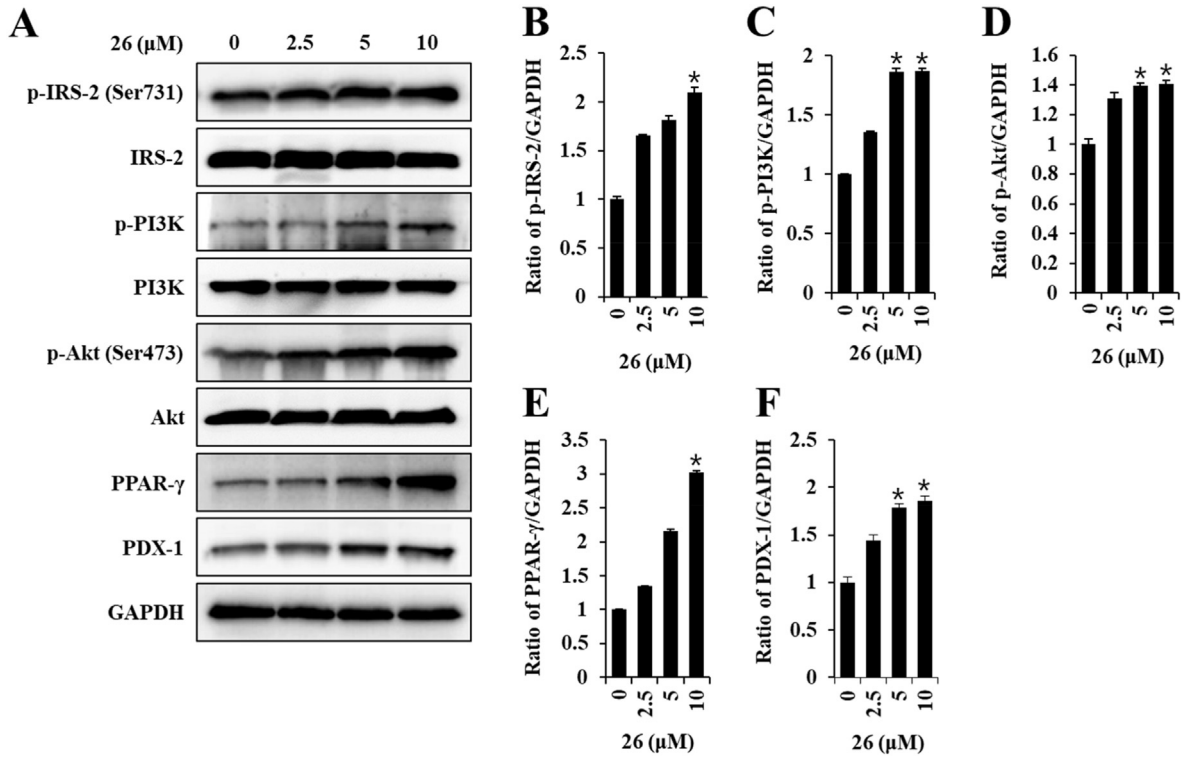

Fig. 2. Effect of **26** on the protein expression of phospho-insulin receptor substrate-2 (p-IRS-2) (Ser731), IRS-2, phospho-phosphatidylinositol 3-kinase (p-PI3K), PI3K, phospho-Akt (p-Akt) (Ser473), Akt, peroxisome proliferator-activated receptor-γ (PPARγ), and pancreatic and duodenal homeobox-1 (PDX-1) in INS-1 cells. (A) Protein expression levels of p-IRS-2 (Ser731), IRS-2, p-PI3K, PI3K, p-Akt (Ser473), Akt, PPAR-γ, PDX-1, and glyceraldehyde 3-phosphate dehydrogenase (GAPDH) in INS-1 cells treated with 0 μM, 2.5 μM, 5 μM, and 10 μM of **26** for 24 h. (B–F) Bar graph presents the densitometric quantification of western blot bands. The experiment was performed in triplicate, and the error bars represent the standard deviation of samples (n = 3). *p < 0.05 compared with the control.

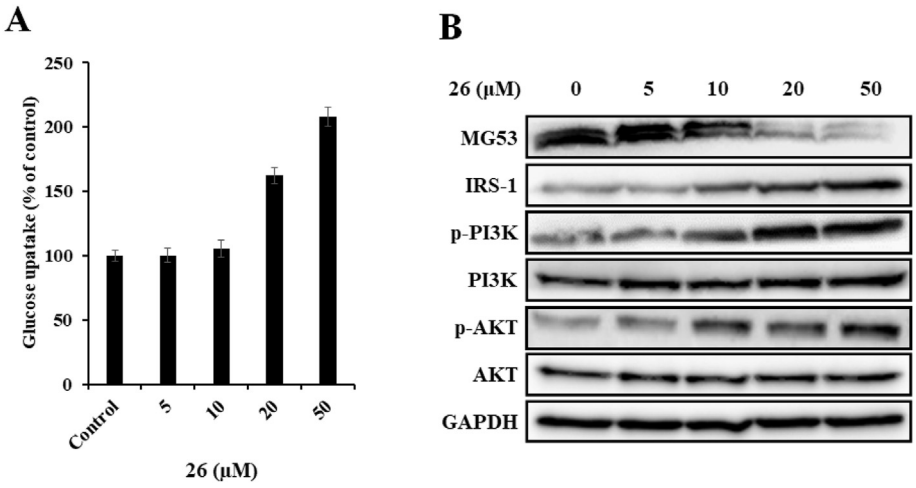

Fig. 3. Effect of **26** on glucose uptake in C2C12 myotube cells. (A) Basal glucose uptake in **26**-treated C2C12 myotubes under normal conditions. (B) Protein expression levels of MG53, IRS-1, p-PI3K, PI3K, p-Akt, Akt, and GAPDH in C2C12 cells treated with 0 μM, 5 μM, 10 μM, 20 μM, and 50 μM of **26** for 16 h.

mechanism underlying glucose transportation regulated by **26**, we further investigated the expression of PI3K/Akt pathway proteins. As displayed Fig. 3B, treatment with **26** increased the levels of PI3K and Akt phosphoproteins, which suggests that **26** has a capacity to stimulate PI3K/Akt signaling in the two different types of cell lines, myotube cells and pancreatic β-cells. To uncover the upstream of PI3K/Akt signaling in response to **26**, the expression of additional proteins was investigated, considering that IRS-1 is one of the most common effectors of the PI3K/Akt signaling pathway in skeletal muscle [38,39]. In Fig. 3B, the expression of IRS-1 was elevated as the concentration of the **26** was increased. However, the expression of Mitsugumin 53 (MG53), which is a ubiquitin E3 ligase that induces IRS-1 degradation in skeletal muscle [39,40], was concentration-dependently suppressed by **26**. Therefore, these results suggest that compound **26** could decrease the expression of MG53 and interfere with MG53-induced IRS-1 ubiquitination, which result in the activation of the IRS-1/PI3K/Akt pathway and the upregulation of glucose uptake. The bi-functionality of **26** could

provide a novel class of antidiabetic therapy that have a potential to reduce blood glucose levels through both insulin secretion in β-cells and glucose uptake in muscle cells.

3. Conclusions

In summary, a novel series of 3-benzyl-*N*-phenyl-1*H*-pyrazole-5-carboxamides was synthesized and evaluated for their glucose-stimulated insulin secretion activity in INS-1 cell line. The newly synthesized 41 analogues were screened for their cytotoxicity against β-cells to ensure pharmaceutical safety. Stepwise SAR-based optimization led to the discovery of compound **26**, which potently increased GSIS from β-cells without cytotoxicity. Western blot assay showed that **26** could augment GSIS via the regulation of PDX-1 activity. In addition, we found that **26** stimulates glucose uptake in C2C12 myotube cells through suppression of MG53 expression. The unique combination of pharmacological actions could provide a novel class of antidiabetic agents that affect the key pathogenic mechanisms in diabetes. Given the bifunctional anti-diabetic effects of **26** and its protein expression profiles, further studies are underway to identify the molecular target of the compound.

4. Materials and methods

4.1. Chemistry

Unless noted otherwise, all starting materials and reagents were obtained from commercial suppliers and were used without further purification. Reaction flasks were dried at 100 °C. Air- and moisture-sensitive reactions were performed under an argon atmosphere. All solvents used for routine isolation of products and chromatography were reagent-grade. Flash column chromatography was performed using silica gel 60 (230–400 mesh, Merck) with the indicated solvents. Thin-layer chromatography was performed using 0.25 mm silica gel plates (Merck). ^{1}H and ^{13}C NMR spectra were recorded on Varian Unity 400, AVANCE NEO 500, and Unity-Inova 500 as solutions in the indicated solvents. Chemical shifts were expressed in parts per million (ppm, δ) downfield from tetramethylsilane and were referenced to the deuterated solvent. ^{1}H NMR data were reported in the order of chemical shift, multiplicity (s, singlet; brs, broad singlet; d, doublet; dd, doublet of doublets; t, triplet; td, triplet of doublets; q, quartet; qd, quartet of doublets; m, multiplet and/or multiple resonance), number of protons, and coupling constant in hertz (Hz). High-resolution mass spectra were obtained with an Agilent 6530 Accurate-Mass Q-TOF and a JEOL JMS-AX 505WA instrument.

4.1.1. General procedures for the preparation of ***3a*-*3e***

To a stirred solution of phenylacetone in toluene was added *t*-BuOK (1.2 equiv. of a 1.0 M solution in THF) at 0 °C. After stirring for 30 min at the same temperature, to the reaction mixture was added diethyl oxalate (1.1 equiv.). The resulting mixture was stirred for 12 h at ambient temperature and quenched with saturated aqueous NH_4Cl. The reaction mixture was extracted with EtOAc and the combined organic layers were dried over $MgSO_4$ and then concentrated in vacuo. The residue was purified by flash column chromatography on silica gel.

*4.1.1.1. Ethyl 5-(4-chlorophenyl)-2,4-dioxopentanoate (**3a**).* 4-Chlorophenylacetone (**2a**) (12.1 g, 71.7 mmol) afforded 18.6 g (97%) of **3a** as a dark red oil. **3a** was purified by flash column chromatography on silica gel (EtOAc: *n*-hexane = 1 : 7 to 1 : 2): ^{1}H NMR ($CDCl_3$, 400 MHz) δ 7.32 (d, 2H, J = 8.1 Hz, Ar−H), 7.17 (d, 2H, J = 8.2 Hz, Ar−H), 6.35 (d, 1H, J = 0.7 Hz, CH), 4.33 (qd, 2H, J = 7.1, 0.6 Hz, $O\underline{CH_2}CH_3$), 3.74 (s, 2H, Ar−CH_2), 1.35 (td, 3H, J = 7.1, 0.7 Hz, $OCH_2\underline{CH_3}$); ^{13}C NMR ($CDCl_3$, 100 MHz) δ 200.1, 166.9, 161.9, 133.6, 132.1, 130.9, 129.2, 101.7, 62.8, 47.0, 14.1; LR-MS (ESI+) *m*/*z* 269 [M + H]$^+$; HR-MS (ESI+) calcd for $C_{13}H_{14}ClO_4$ [M + H]$^+$ 269.0575; found 269.0574.

*4.1.1.2. Ethyl 5-(4-fluorophenyl)-2,4-dioxopentanoate (**3b**).* 4-Fluorophenylacetone (**2b**) (1.19 g, 7.82 mmol) afforded 1.38 g (67%) of **3b** as an orange oil. **3b** was purified by flash column chromatography on silica gel (EtOAc: *n*-hexane = 1 : 7): ^{1}H NMR ($CDCl_3$, 500 MHz) δ 7.21 (dd, 2H, J = 8.3, 5.4 Hz, Ar−H), 7.04 (t, 2H, J = 8.6 Hz, Ar−H), 6.35 (s, 1H, CH), 4.33 (q, 2H, J = 7.1 Hz, $O\underline{CH_2}CH_3$), 3.75 (s, 2H, Ar−CH_2), 1.36 (t, 3H, J = 7.1 Hz, $OCH_2\underline{CH_3}$); ^{13}C NMR ($CDCl_3$, 125 MHz) δ 200.4, 167.0, 163.3, 162.0, 161.4, 131.2, 131.1, 129.4, 129.4, 116.1, 115.9, 101.6, 62.8, 46.9, 14.2; LR-MS (ESI+) *m*/*z* 253 [M + H]$^+$; HR-MS (ESI+) calcd for $C_{13}H_{14}FO_4$ [M + H]$^+$ 253.0871; found 253.0874.

*4.1.1.3. Ethyl 5-(4-methoxyphenyl)-2,4-dioxopentanoate (**3c**).* 4-Methoxyphenylacetone (**2c**) (5.06 g, 30.8 mmol) afforded 5.73 g (70%) of **3c** as a dark orange oil. **3c** was purified by flash column chromatography on silica gel (EtOAc: *n*-hexane = 1 : 7): ^{1}H NMR ($CDCl_3$, 400 MHz) δ 7.15 (d, 2H, J = 8.3 Hz, Ar−H), 6.88 (d, 2H, J = 8.8 Hz, Ar−H), 6.35 (s, 1H, CH), 4.31 (q, 2H, J = 7.1 Hz, $O\underline{CH_2}CH_3$), 3.79 (s, 3H, OCH_3), 3.70 (s, 2H, Ar−CH_2), 1.34 (t, 3H, J = 7.2 Hz, $OCH_2\underline{CH_3}$); ^{13}C NMR ($CDCl_3$, 125 MHz) δ 201.2, 166.8, 162.1, 159.1, 130.6, 125.7, 114.5, 101.7, 62.7, 55.4, 47.0, 14.2; DEPT 90 ($CDCl_3$, 125 MHz) δ 130.6, 114.5, 101.7; DEPT 135 ($CDCl_3$, 125 MHz) δ 130.6, 114.5, 101.7, 62.7 (−), 55.4, 47.0 (−), 14.2; LR-MS (ESI+) *m*/*z* 287 [M + Na]$^+$; HR-MS (ESI+) calcd for $C_{14}H_{16}NaO_5$ [M + Na]$^+$ 287.0890; found 287.0879.

*4.1.1.4. Ethyl 5-(3-chlorophenyl)-2,4-dioxopentanoate (**3d**).* 3-Chlorophenylacetone (**2d**) (200 mg, 1.54 mmol) afforded 254 mg (61%) of **3d** as a colorless oil. **3d** was purified by flash column chromatography on silica gel (EtOAc: *n*-hexane = 1 : 7): ^{1}H NMR ($CDCl_3$, 500 MHz) δ 7.27 (m, 3H, Ar−H), 7.13 (m, 1H, Ar−H), 6.36 (s, 1H, CH), 4.34 (q, 2H, J = 7.1 Hz, $O\underline{CH_2}CH_3$), 3.75 (s, 2H, Ar−CH_2), 1.36 (t, 3H, J = 7.1 Hz, $OCH_2\underline{CH_3}$); ^{13}C NMR ($CDCl_3$, 125 MHz) δ 199.7, 167.1, 161.9, 135.6, 134.8, 130.2, 129.7, 127.9, 127.8, 101.7, 62.8, 47.2, 14.1; DEPT 90 ($CDCl_3$, 125 MHz) δ 130.2, 129.7, 127.9, 127.8, 101.7; DEPT 135 ($CDCl_3$, 125 MHz) δ 130.2, 129.7, 127.9, 127.8, 101.7, 62.8 (−), 47.2 (−), 14.1; LR-MS (ESI+) *m*/*z* 269 [M + H]$^+$; HR-MS (ESI+) calcd for $C_{13}H_{14}ClO_4$ [M + H]$^+$ 269.0575; found 269.0583.

*4.1.1.5. Ethyl 5-(2-chlorophenyl)-2,4-dioxopentanoate (**3e**).* 2-Chlorophenylacetone (**2e**) (200 mg, 1.54 mmol) afforded 316 mg (77%) of **3e** as a pale yellow oil. **3e** was purified by flash column chromatography on silica gel (EtOAc: *n*-hexane = 1 : 4): ^{1}H NMR ($CDCl_3$, 500 MHz) δ 7.41 (m, 1H, Ar−H), 7.26 (m, 3H, Ar−H), 6.37 (s, 1H, CH), 4.33 (q, 2H, J = 7.1 Hz, $O\underline{CH_2}CH_3$), 3.95 (s, 2H, Ar−CH_2), 1.35 (t, 3H, J = 7.2 Hz, $OCH_2\underline{CH_3}$); ^{13}C NMR ($CDCl_3$, 125 MHz) δ 200.3, 165.8, 162.1, 134.7, 132.1, 131.9, 129.9, 129.3, 127.3, 101.9, 62.7, 45.7, 14.2; LR-MS (ESI+) *m*/*z* 269 [M + H]$^+$; HR-MS (ESI+) calcd for $C_{13}H_{14}ClO_4$ [M + H]$^+$ 269.0575; found 269.0577.

4.1.2. General procedures for the preparation of ***4a*-*4e***

To a stirred solution of 2,4-dioxopentanoate in acetic acid was added hydrazine monohydrate (2.0 equiv.) at ambient temperature. After stirring for 12 h, the reaction mixture was quenched with saturated aqueous $NaHCO_3$ and then extracted with EtOAc. The combined organic layers were dried over $MgSO_4$ and concentrated in vacuo. The residue was purified by flash column chromatography on silica gel.

*4.1.2.1. Ethyl 3-(4-chlorobenzyl)-1H-pyrazole-5-carboxylate (**4a**).* Ethyl 5-(4-chlorophenyl)-2,4-dioxopentanoate (**3a**) (2.47 g, 9.20 mmol) afforded 2.26 g (93%) of **4a** as a dark red oil. **4a** was purified by flash column chromatography on silica gel (EtOAc: *n*-hexane = 1 : 3): ^{1}H NMR ($CDCl_3$, 400 MHz) δ 11.31 (brs, 1H, NH), 7.27 (d, 2H, J = 8.4 Hz, Ar−H), 7.15 (d, 2H, J = 8.4 Hz, Ar−H), 6.56 (s, 1H, pyrazole−H), 4.35 (q, 2H, J = 7.1 Hz, O$\underline{CH_2}CH_3$), 4.01 (s, 2H, Ar−CH_2), 1.36 (t, 3H, J = 7.1 Hz, $OCH_2\underline{CH_3}$); ^{13}C NMR ($CDCl_3$, 100 MHz) δ 161.3, 148.1, 139.9, 136.9, 132.6, 130.2, 128.9, 107.5, 61.3, 32.6, 14.4; LR-MS (ESI+) *m/z* 265 $[M + H]^+$; HR-MS (ESI+) calcd for $C_{13}H_{14}ClN_2O_2$ $[M + H]^+$ 265.0738; found 265.0736.

*4.1.2.2. Ethyl 3-(4-fluorobenzyl)-1H-pyrazole-5-carboxylate (**4b**).* Ethyl 5-(4-fluorophenyl)-2,4-dioxopentanoate (**3b**) (2.25 g, 8.92 mmol) afforded 1.48 g (67%) of **4b** as a yellow oil. **4b** was purified by flash column chromatography on silica gel (EtOAc: *n*-hexane = 1 : 3): ^{1}H NMR ($CDCl_3$, 400 MHz) δ 7.17 (dd, 2H, J = 8.4, 5.4 Hz, Ar−H), 6.97 (t, 2H, J = 8.6 Hz, Ar−H), 6.54 (s, 1H, pyrazole−H), 4.33 (q, 2H, J = 7.1 Hz, O$\underline{CH_2}CH_3$), 4.02 (s, 2H, Ar−CH_2), 1.33 (t, 3H, J = 7.1 Hz, $OCH_2\underline{CH_3}$); ^{13}C NMR ($CDCl_3$, 100 MHz) δ 163.0, 161.2, 160.6, 148.6, 139.7, 134.1, 134.0, 130.3, 130.2, 115.7, 115.5, 107.6, 61.3, 32.5, 14.4; LR-MS (ESI+) *m/z* 249 $[M + H]^+$; HR-MS (ESI+) calcd for $C_{13}H_{14}FN_2O_2$ $[M + H]^+$ 249.1034; found 249.1036.

*4.1.2.3. Ethyl 3-(4-methoxybenzyl)-1H-pyrazole-5-carboxylate (**4c**).* Ethyl 5-(4-methoxyphenyl)-2,4-dioxopentanoate (**3c**) (3.47 g, 13.1 mmol) afforded 3.10 g (91%) of **4c** as an orange oil. **4c** was purified by flash column chromatography on silica gel (EtOAc: *n*-hexane = 1 : 3): ^{1}H NMR ($CDCl_3$, 500 MHz) δ 7.13 (d, 2H, J = 8.5 Hz, Ar−H), 6.83 (d, 2H, J = 8.6 Hz, Ar−H), 6.55 (s, 1H, pyrazole−H), 4.34 (q, 2H, J = 7.1 Hz, O$\underline{CH_2}CH_3$), 3.98 (s, 2H, Ar−CH_2), 3.78 (s, 3H, OCH_3), 1.34 (t, 3H, J = 7.1 Hz, $OCH_2\underline{CH_3}$); ^{13}C NMR ($CDCl_3$, 100 MHz) δ 161.2, 158.6, 149.1, 140.0, 130.2, 129.8, 114.3, 107.5, 61.3, 55.4, 32.5, 14.4; LR-MS (ESI+) *m/z* 261 $[M + H]^+$; HR-MS (ESI+) calcd for $C_{14}H_{17}N_2O_3$ $[M + H]^+$ 261.1234; found 261.1231.

*4.1.2.4. Ethyl 3-(3-chlorobenzyl)-1H-pyrazole-5-carboxylate (**4d**).* Ethyl 5-(3-chlorophenyl)-2,4-dioxopentanoate (**3d**) (2.60 g, 9.68 mmol) afforded 1.78 g (69%) of **4d** as red solid. **4d** was purified by flash column chromatography on silica gel (EtOAc: *n*-hexane = 1 : 3): ^{1}H NMR ($CDCl_3$, 500 MHz) δ 12.01 (brs, 1H, NH), 7.20 (m, 3H, Ar−H), 7.09 (m, 1H, Ar−H), 6.56 (s, 1H, pyrazole−H), 4.34 (q, 2H, J = 7.1 Hz, O$\underline{CH_2}CH_3$), 4.03 (s, 2H, Ar−CH_2), 1.33 (t, 3H, J = 7.1 Hz, $OCH_2\underline{CH_3}$); ^{13}C NMR ($CDCl_3$, 100 MHz) δ 161.2, 148.2, 140.6, 139.7, 134.6, 130.0, 129.0, 127.0, 127.0, 107.7, 61.3, 33.0, 14.4; LR-MS (ESI+) *m/z* 265 $[M + H]^+$; HR-MS (ESI+) calcd for $C_{13}H_{14}ClN_2O_2$ $[M + H]^+$ 265.0738; found 265.0739.

*4.1.2.5. Ethyl 3-(2-chlorobenzyl)-1H-pyrazole-5-carboxylate (**4e**).* Ethyl 5-(2-chlorophenyl)-2,4-dioxopentanoate (**3e**) (316 mg, 1.18 mmol) afforded 246 mg (79%) of **4e** as an orange oil. **4e** was purified by flash column chromatography on silica gel (EtOAc: *n*-hexane = 1 : 4): ^{1}H NMR ($CDCl_3$, 500 MHz) δ 8.15 (brs, 1H, NH), 7.38 (m, 1H, Ar−H), 7.25 (m, 1H, Ar−H), 7.20 (m, 2H, Ar−H), 6.60 (s, 1H, pyrazole−H), 4.35 (q, 2H, J = 7.1 Hz, O$\underline{CH_2}CH_3$), 4.19 (s, 2H, Ar−CH_2), 1.35 (t, 3H, J = 7.2 Hz, $OCH_2\underline{CH_3}$); ^{13}C NMR ($CDCl_3$, 125 MHz) δ 160.9, 147.5, 139.6, 136.1, 134.1, 130.9, 129.8, 128.5, 127.3, 107.9, 61.4, 31.1, 14.4; LR-MS (ESI+) *m/z* 265 $[M + H]^+$; HR-MS (ESI+) calcd for $C_{13}H_{14}ClN_2O_2$ $[M + H]^+$ 265.0738; found 265.0739.

*4.1.3. General procedures for the preparation of **5a-5e**, **45**, and **48***

To a stirred solution of 1*H*-pyrazole-5-carboxylate in THF was added a solution of $LiOH\cdot H_2O$ (2.0 equiv.) in H_2O at ambient temperature. After stirring for 6 h at 50 °C, the reaction mixture was acidified with 2 N HCl then extracted with EtOAc. The combined organic layers were dried over $MgSO_4$ and concentrated in vacuo. The residue was purified by flash column chromatography on silica gel.

*4.1.3.1. 3-(4-Chlorobenzyl)-1H-pyrazole-5-carboxylic acid (**5a**).* Ethyl 3-(4-chlorobenzyl)-1*H*-pyrazole-5-carboxylate (**4a**) (10.3 g, 39.0 mmol) afforded 8.24 g (89%) of **5a** as pale yellow solid. **5a** was purified by flash column chromatography on silica gel (EtOAc: *n*-hexane = 1 : 2 to MeOH: EtOAc = 1 : 10): ^{1}H NMR (DMSO-d_6, 400 MHz) δ 7.34 (d, 2H, J = 7.6 Hz, Ar−H), 7.26 (d, 2H, J = 7.5 Hz, Ar−H), 6.30 (s, 1H, pyrazole−H), 3.92 (s, 2H, Ar−CH_2); ^{13}C NMR (DMSO-d_6, 100 MHz) δ 162.3, 146.6, 140.3, 138.3, 131.0, 130.4, 128.4, 106.9, 31.5; LR-MS (ESI+) *m/z* 237 $[M + H]^+$; HR-MS (ESI+) calcd for $C_{11}H_{10}ClN_2O_2$ $[M + H]^+$ 237.0425; found 237.0424.

*4.1.3.2. 3-(4-Fluorobenzyl)-1H-pyrazole-5-carboxylic acid (**5b**).* Ethyl 3-(4-fluorobenzyl)-1*H*-pyrazole-5-carboxylate (**4b**) (990 mg, 3.99 mmol) afforded 766 mg (87%) of **5b** as white solid. **5b** was purified by flash column chromatography on silica gel (EtOAc: *n*-hexane = 1 : 2 to MeOH: EtOAc = 1 : 10): ^{1}H NMR (DMSO-d_6, 400 MHz) δ 7.28 (t, 2H, J = 6.1 Hz, Ar−H), 7.12 (t, 2H, J = 8.1 Hz, Ar−H), 6.40 (s, 1H, pyrazole−H), 3.94 (s, 2H, Ar−CH_2); ^{13}C NMR (DMSO-d_6, 100 MHz) δ 162.1, 159.7, 147.2, 141.4, 135.6, 130.4, 130.3, 115.2, 115.0, 106.3, 31.5; LR-MS (ESI+) *m/z* 221 $[M + H]^+$; HR-MS (ESI+) calcd for $C_{11}H_{10}FN_2O_2$ $[M + H]^+$ 221.0721; found 221.0724.

*4.1.3.3. 3-(4-Methoxybenzyl)-1H-pyrazole-5-carboxylic acid (**5c**).* Ethyl 3-(4-methoxybenzyl)-1*H*-pyrazole-5-carboxylate (**4c**) (2.28 g, 8.76 mmol) afforded 1.45 g (71%) of **5c** as white solid. **5c** was purified by flash column chromatography on silica gel (EtOAc: *n*-hexane = 1 : 2 to MeOH: EtOAc = 1 : 10): ^{1}H NMR (DMSO-d_6, 400 MHz) δ 7.15 (d, 2H, J = 8.6 Hz, Ar−H), 6.86 (d, 2H, J = 8.7 Hz, Ar−H), 6.40 (s, 1H, pyrazole−H), 3.87 (s, 2H, Ar−CH_2), 3.71 (s, 3H, OCH_3); ^{13}C NMR (DMSO-d_6, 100 MHz) δ 162.6, 157.8, 147.1, 141.0, 131.1, 129.5, 113.9, 106.5, 55.0, 31.2; LR-MS (ESI+) *m/z* 233 $[M + H]^+$; HR-MS (ESI+) calcd for $C_{12}H_{13}N_2O_3$ $[M + H]^+$ 233.0921; found 233.0923.

*4.1.3.4. 3-(3-Chlorobenzyl)-1H-pyrazole-5-carboxylic acid (**5d**).* Ethyl 3-(3-chlorobenzyl)-1*H*-pyrazole-5-carboxylate (**4d**) (180 mg, 0.680 mmol) afforded 153 mg (95%) of **5d** as a colorless oil. **5d** was recrystallized with EtOAc/*n*-hexane: ^{1}H NMR (DMSO-d_6, 500 MHz) δ 13.10 (brs, 1H, NH), 7.33 (t, 1H, J = 7.4 Hz, Ar−H), 7.32 (s, 1H, Ar−H), 7.27 (d, 1H, J = 8.2 Hz, Ar−H), 7.21 (d, 1H, J = 7.6 Hz, Ar−H), 6.51 (s, 1H, pyrazole−H), 3.97 (s, 2H, Ar−CH_2); ^{13}C NMR (DMSO-d_6, 125 MHz) δ 162.2, 146.0, 141.8, 140.3, 133.0, 130.4, 128.4, 127.3, 126.3, 107.0, 31.7; LR-MS (ESI+) *m/z* 237 $[M + H]^+$; HR-MS (ESI+) calcd for $C_{11}H_{10}ClN_2O_2$ $[M + H]^+$ 237.0425; found 237.0426.

*4.1.3.5. 3-(2-Chlorobenzyl)-1H-pyrazole-5-carboxylic acid (**5e**).* Ethyl 3-(2-chlorobenzyl)-1*H*-pyrazole-5-carboxylate (**4e**) (226 mg, 0.855 mmol) afforded 192 mg (95%) of **5e** as pale yellow solid. **5e** was purified by flash column chromatography on silica gel (EtOAc: *n*-hexane = 1 : 1 to MeOH: EtOAc = 1 : 10): ^{1}H NMR (DMSO-d_6, 500 MHz) δ 13.12 (brs, 1H, NH), 7.45 (m, 1H, Ar−H), 7.32 (m, 1H, Ar−H), 7.29 (m, 2H, Ar−H), 6.40 (s, 1H, pyrazole−H), 4.07 (s, 2H, Ar−CH_2); ^{13}C NMR (DMSO-d_6, 125 MHz) δ 162.3, 145.8, 140.4, 136.7, 132.9, 131.0, 129.3, 128.5, 127.4, 106.9, 30.2; LR-MS (ESI+) *m/z* 237 $[M + H]^+$; HR-MS (ESI+) calcd for $C_{11}H_{10}ClN_2O_2$ $[M + H]^+$ 237.0425; found 237.0422.

*4.1.3.6. 3-(4-Chlorobenzyl)-1-methyl-1H-pyrazole-5-carboxylic acid (**45**).* Ethyl 3-(4-chlorobenzyl)-1-methyl-1*H*-pyrazole-5-carboxylate (**44**) (237 mg, 0.850 mmol) afforded 202 mg (95%) of **45** as pale yellow solid. **45** was purified by flash column

chromatography on silica gel (EtOAc to MeOH: EtOAc = 1 : 1): ^{1}H NMR (DMSO-d_6, 500 MHz) δ 7.34 (d, 2H, J = 8.4 Hz, Ar−H), 7.26 (d, 2H, J = 8.3 Hz, Ar−H), 6.55 (s, 1H, pyrazole−H), 4.00 (s, 3H, CH_3), 3.87 (s, 2H, Ar−CH_2), 3.34 (brs, 1H, COOH); ^{13}C NMR (DMSO-d_6, 125 MHz) δ 160.8, 149.1, 138.9, 134.1, 130.7, 130.5, 128.3, 109.6, 38.8, 32.8; LR-MS (ESI+) m/z 251 $[M + H]^+$; HR-MS (ESI+) calcd for $C_{12}H_{12}ClN_2O_2$ $[M + H]^+$ 251.0582; found 251.0583.

*4.1.3.7. 3-(4-Chlorobenzoyl)-1H-pyrazole-5-carboxylic acid (**48**).* Ethyl 3-(4-chlorobenzoyl)-1*H*-pyrazole-5-carboxylate (**47**) (645 mg, 2.31 mmol) afforded 534 mg (92%) of **48** as white solid. **48** was purified by flash column chromatography on silica gel (MeOH: CH_2Cl_2 = 1 : 10): ^{1}H NMR (DMSO-d_6, 500 MHz) δ 8.17 (s, 2H, Ar−H), 7.63 (d, 2H, J = 8.5 Hz, Ar−H), 7.26 (s, 1H, pyrazole−H); ^{13}C NMR (DMSO-d_6, 125 MHz) δ 185.3, 160.5, 150.6, 138.0, 137.1, 135.3, 131.9, 128.6, 111.0; LR-MS (ESI+) m/z 251 $[M + H]^+$; HR-MS (ESI+) calcd for $C_{11}H_8ClN_2O_3$ $[M + H]^+$ 251.0218; found 251.0219.

*4.1.4. General procedures for the preparation of **1** and **6**–**42***

To a stirred solution of carboxylic acid and aniline in CH_2Cl_2 were added EDC·HCl (2.0 equiv.) and DMAP (0.1 equiv.) at ambient temperature. After stirring for 2 h, the reaction mixture was quenched with H_2O and then extracted with CH_2Cl_2. The combined organic layer was dried over $MgSO_4$ and concentrated in vacuo. The residue was purified by flash column chromatography on silica gel.

*4.1.4.1. 3-(4-chlorobenzyl)-N-(4-fluorophenyl)-1H-pyrazole-5-carboxamide (**1**).* 3-(4-Chlorobenzyl)-1*H*-pyrazole-5-carboxylic acid (**5a**) (45.4 mg, 0.192 mmol) and 4-fluoroaniline (18.2 μL, 0.192 mmol) afforded 32.1 mg (51%) of **1** as pale yellow solid. **1** was purified by flash column chromatography on silica gel (EtOAc: *n*-hexane = 1 : 2 to 1 : 1): ^{1}H NMR (DMSO-d_6, 400 MHz) δ 10.08 (s, 1H, NH), 7.77 (m, 2H, Ar−H), 7.38 (d, 2H, J = 8.2 Hz, Ar−H), 7.29 (d, 2H, J = 8.4 Hz, Ar−H), 7.15 (t, 2H, J = 8.8 Hz, Ar−H), 6.53 (s, 1H, pyrazole−H), 4.01 (s, 2H, Ar−CH_2); ^{13}C NMR (DMSO-d_6, 100 MHz) δ 160.6, 159.5, 157.1, 146.9, 143.7, 138.0, 135.2, 131.2, 130.5, 128.6, 122.2, 122.1, 115.4, 115.1, 104.9, 30.4; LR-MS (ESI+) m/z 330 $[M + H]^+$; HR-MS (ESI+) calcd for $C_{17}H_{14}ClFN_3O$ $[M + H]^+$ 330.0804; found 330.0801.

*4.1.4.2. 3-(4-Chlorobenzyl)-N-phenyl-1H-pyrazole-5-carboxamide (**6**).* 3-(4-Chlorobenzyl)-1*H*-pyrazole-5-carboxylic acid (**5a**) (48.2 mg, 0.204 mmol) and aniline (18.6 μL, 0.204 mmol) afforded 22.3 mg (35%) of **6** as pale yellow solid. **6** was purified by flash column chromatography on silica gel (EtOAc: *n*-hexane = 1 : 2 to 1 : 1): ^{1}H NMR (DMSO-d_6, 400 MHz) δ 13.26 (s, 1H, NH), 9.94 (s, 1H, NH), 7.78 (d, 2H, J = 8.0 Hz, Ar−H), 7.38 (d, 2H, J = 8.5 Hz, Ar−H), 7.30 (d, 2H, J = 6.0 Hz, Ar−H), 7.28 (d, 2H, J = 8.2 Hz, Ar−H), 7.04 (t, 1H, J = 7.2 Hz, Ar−H), 6.51 (s, 1H, pyrazole−H), 4.02 (s, 2H, Ar−CH_2); ^{13}C NMR (DMSO-d_6, 100 MHz) δ 160.4, 147.1, 143.5, 138.8, 137.7, 131.1, 130.3, 128.5, 128.5, 123.3, 120.1, 104.7, 30.2; LR-MS (ESI+) m/z 312 $[M + H]^+$; HR-MS (ESI+) calcd for $C_{17}H_{15}ClN_3O$ $[M + H]^+$ 312.0898; found 312.0897.

*4.1.4.3. N-(4-(tert-Butyl)phenyl)-3-(4-chlorobenzyl)-1H-pyrazole-5-carboxamide (**7**).* 3-(4-Chlorobenzyl)-1*H*-pyrazole-5-carboxylic acid (**5a**) (48.9 mg, 0.207 mmol) and 4-*t*-butylaniline (33.0 μL, 0.207 mmol) afforded 20.3 mg (27%) of **7** as pale yellow solid. **7** was purified by flash column chromatography on silica gel (EtOAc: *n*-hexane = 1 : 2 to 1 : 1): ^{1}H NMR (DMSO-d_6, 400 MHz) δ 13.24 (s, 1H, NH), 9.86 (s, 1H, NH), 7.67 (d, 2H, J = 8.8 Hz, Ar−H), 7.37 (d, 2H, J = 8.0 Hz, Ar−H), 7.30 (d, 2H, J = 7.8 Hz, Ar−H), 7.28 (d, 2H, J = 8.2 Hz, Ar−H), 6.50 (s, 1H, pyrazole−H), 4.01 (s, 2H, Ar−CH_2), 1.24 (s, 9H, $(CH_3)_3$); ^{13}C NMR (DMSO-d_6, 100 MHz) δ 160.5, 147.4, 145.8, 143.6, 137.9, 136.5, 131.4, 130.5, 128.7, 125.3, 120.1, 104.9, 34.2, 31.4, 30.4; LR-MS (ESI+) m/z 368 $[M + H]^+$; HR-MS (ESI+) calcd for $C_{21}H_{23}ClN_3O$ $[M + H]^+$ 368.1524; found 368.1529.

*4.1.4.4. 3-(4-Chlorobenzyl)-N-(4-(trifluoromethyl)phenyl)-1H-pyrazole-5-carboxamide (**8**).*
3-(4-Chlorobenzyl)-1*H*-pyrazole-5-carboxylic acid (**5a**) (60.4 mg, 0.255 mmol) and 4-(trifluoromethyl)aniline (32.8 μL, 0.255 mmol) afforded 17.1 mg (18%) of **8** as pale yellow solid. **8** was purified by flash column chromatography on silica gel (EtOAc: *n*-hexane = 1 : 4): ^{1}H NMR (DMSO-d_6, 400 MHz) δ 13.36 (s, 1H, NH), 10.39 (s, 1H, NH), 8.04 (d, 2H, J = 8.4 Hz, Ar−H), 7.67 (d, 2H, J = 8.4 Hz, Ar−H), 7.39 (d, 2H, J = 7.5 Hz, Ar−H), 7.29 (d, 2H, J = 8.2 Hz, Ar−H), 6.56 (s, 1H, pyrazole−H), 4.04 (s, 2H, Ar−CH_2); ^{13}C NMR (DMSO-d_6, 100 MHz) δ 161.1, 146.9, 143.9, 142.8, 137.9, 131.4, 130.8, 130.6, 128.7, 128.6, 126.3, 126.1, 126.0, 124.0, 123.7, 123.3, 123.0, 120.2, 105.2, 30.4; LR-MS (ESI+) m/z 380 $[M + H]^+$; HR-MS (ESI+) calcd for $C_{18}H_{14}ClF_3N_3O$ $[M + H]^+$ 380.0772; found 380.0786.

*4.1.4.5. 3-(4-Chlorobenzyl)-N-(4-methoxyphenyl)-1H-pyrazole-5-carboxamide (**9**).* 3-(4-Chlorobenzyl)-1*H*-pyrazole-5-carboxylic acid (**5a**) (45.1 mg, 0.190 mmol) and 4-methoxyaniline (23.4 mg, 0.190 mmol) afforded 23.9 mg (37%) of **9** as white solid. **9** was purified by flash column chromatography on silica gel (EtOAc: *n*-hexane = 1 : 2 to 1 : 1): ^{1}H NMR (DMSO-d_6, 400 MHz) δ 13.24 (s, 1H, NH), 9.84 (s, 1H, NH), 7.68 (d, 2H, J = 7.4 Hz, Ar−H), 7.38 (d, 2H, J = 7.8 Hz, Ar−H), 7.29 (d, 2H, J = 7.4 Hz, Ar−H), 6.88 (d, 2H, J = 8.1 Hz, Ar−H), 6.50 (s, 1H, pyrazole−H), 4.02 (s, 2H, Ar−CH_2), 3.73 (s, 3H, OCH_3); ^{13}C NMR (DMSO-d_6, 100 MHz) δ 160.2, 155.3, 147.2, 143.4, 137.7, 132.0, 131.2, 130.4, 128.5, 121.7, 113.7, 104.5, 55.2, 30.3; LR-MS (ESI+) m/z 342 $[M + H]^+$; HR-MS (ESI+) calcd for $C_{18}H_{17}ClN_3O_2$ $[M + H]^+$ 342.1004; found 342.1007.

*4.1.4.6. Methyl 4-(3-(4-chlorobenzyl)-1H-pyrazole-5-carboxamido) benzoate (**10**).* 3-(4-Chlorobenzyl)-1*H*-pyrazole-5-carboxylic acid (**5a**) (102 mg, 0.431 mmol) and methyl 4-aminobenzoate (65.1 mg, 0.431 mmol) afforded 70.2 mg (44%) of **10** as pale yellow solid. **10** was purified by flash column chromatography on silica gel (EtOAc: *n*-hexane = 1 : 2 to 2 : 1): ^{1}H NMR (DMSO-d_6, 400 MHz) δ 13.37 (s, 1H, NH), 10.36 (s, 1H, NH), 7.97 (d, 2H, J = 8.8 Hz, Ar−H), 7.91 (d, 2H, J = 8.5 Hz, Ar−H), 7.39 (d, 2H, J = 7.9 Hz, Ar−H), 7.30 (d, 2H, J = 7.9 Hz, Ar−H), 6.55 (s, 1H, pyrazole−H), 4.04 (s, 2H, Ar−CH_2), 3.82 (s, 3H, $COOCH_3$); ^{13}C NMR (DMSO-d_6, 100 MHz) δ 165.9, 160.9, 146.7, 143.7, 143.5, 137.7, 131.2, 130.4, 130.1, 128.6, 124.0, 119.5, 105.0, 52.0, 30.2; LR-MS (ESI+) m/z 370 $[M + H]^+$; HR-MS (ESI+) calcd for $C_{19}H_{17}ClN_3O_3$ $[M + H]^+$ 370.0953; found 370.0962.

*4.1.4.7. 3-(4-Fluorobenzyl)-N-(4-fluorophenyl)-1H-pyrazole-5-carboxamide (**11**).* 3-(4-Fluorobenzyl)-1*H*-pyrazole-5-carboxylic acid (**5b**) (47.7 mg, 0.217 mmol) and 4-fluoroaniline (20.6 μL, 0.217 mmol) afforded 37.7 mg (55%) of **11** as white solid. **11** was purified by flash column chromatography on silica gel (EtOAc: *n*-hexane = 1 : 2 to 1 : 1): ^{1}H NMR (DMSO-d_6, 400 MHz) δ 13.29 (s, 1H, NH), 10.10 (s, 1H, NH), 7.83 (dd, 2H, J = 9.0, 5.1 Hz, Ar−H), 7.32 (dd, 2H, J = 8.4, 5.6 Hz, Ar−H), 7.17 (dd, 2H, J = 8.9, 3.1 Hz, Ar−H), 7.15 (dd, 2H, J = 8.9, 3.2 Hz, Ar−H), 6.52 (s, 1H, pyrazole−H), 4.03 (s, 2H, Ar−CH_2); ^{13}C NMR (DMSO-d_6, 100 MHz) δ 162.2, 160.5, 159.8, 159.3, 156.9, 147.0, 143.9, 135.3, 135.3, 134.9, 134.8, 130.4, 130.3, 122.0, 121.9, 115.4, 115.2, 115.0, 104.7, 30.1; LR-MS (ESI+) m/z 314 $[M + H]^+$; HR-MS (ESI+) calcd for $C_{17}H_{14}F_2N_3O$ $[M + H]^+$ 314.1099; found 314.1099.

*4.1.4.8. 3-(4-Fluorobenzyl)-N-phenyl-1H-pyrazole-5-carboxamide (**12**).* 3-(4-Fluorobenzyl)-1*H*-pyrazole-5-carboxylic acid (**5b**) (53.6 mg, 0.243 mmol) and aniline (22.1 μL, 0.243 mmol) afforded 40.1 mg (56%) of **12** as white solid. **12** was purified by flash column

chromatography on silica gel (EtOAc: *n*-hexane = 2 : 3 to 3 : 1): ^{1}H NMR (DMSO-d_6, 400 MHz) δ 13.29 (s, 1H, NH), 9.99 (s, 1H, NH), 7.81 (d, 2H, J = 7.8 Hz, Ar−H), 7.33 (m, 2H, Ar−H), 7.29 (m, 2H, Ar−H), 7.15 (t, 2H, J = 8.7 Hz, Ar−H), 7.05 (t, 1H, J = 7.2 Hz, Ar−H), 6.53 (s, 1H, pyrazole−H), 4.03 (s, 2H, Ar−CH_2); ^{13}C NMR (DMSO-d_6, 100 MHz) δ 162.2, 160.6, 159.8, 147.1, 144.0, 138.9, 134.9, 130.4, 130.3, 128.7, 128.6, 123.4, 120.2, 115.4, 115.2, 104.7, 30.1; LR-MS (ESI+) *m/z* 296 [M + H]$^+$; HR-MS (ESI+) calcd for $C_{17}H_{15}FN_3O$ [M + H]$^+$ 296.1194; found 296.1194.

*4.1.4.9. N-(4-(tert-Butyl)phenyl)-3-(4-fluorobenzyl)-1H-pyrazole-5-carboxamide (**13**).* 3-(4-Fluorobenzyl)-1*H*-pyrazole-5-carboxylic acid (**5b**) (62.5 mg, 0.284 mmol) and 4-*t*-butylaniline (45.2 μL, 0.284 mmol) afforded 78.8 mg (79%) of **13** as white solid. **13** was purified by flash column chromatography on silica gel (EtOAc: *n*-hexane = 1 : 3 to 1 : 1): ^{1}H NMR ($CDCl_3$, 400 MHz) δ 11.60 (brs, 1H, NH), 8.80 (s, 1H, NH), 7.54 (d, 2H, J = 8.6 Hz, Ar−H), 7.33 (d, 2H, J = 8.6 Hz, Ar−H), 7.09 (dd, 2H, J = 8.4, 5.4 Hz, Ar−H), 6.91 (t, 2H, J = 8.6 Hz, Ar−H), 6.62 (s, 1H, pyrazole−H), 3.94 (s, 2H, Ar−CH_2), 1.30 (s, 9H, $(CH_3)_3$); ^{13}C NMR ($CDCl_3$, 100 MHz) δ 163.1, 160.6, 160.3, 147.5, 146.8, 145.2, 135.0, 133.2, 133.1, 130.2, 130.2, 126.0, 120.0, 115.8, 115.6, 105.4, 34.5, 31.4, 31.3; LR-MS (ESI+) *m/z* 352 [M + H]$^+$; HR-MS (ESI+) calcd for $C_{21}H_{23}FN_3O$ [M + H]$^+$ 352.1820; found 352.1823.

*4.1.4.10. 3-(4-Fluorobenzyl)-N-(4-(trifluoromethyl)phenyl)-1H-pyrazole-5-carboxamide (**14**).*
3-(4-Fluorobenzyl)-1*H*-pyrazole-5-carboxylic acid (**5b**) (72.0 mg, 0.327 mmol) and 4-(trifluoromethyl)aniline (41.1 μL, 0.327 mmol) afforded 55.9 mg (47%) of **14** as pale yellow solid. **14** was purified by flash column chromatography on silica gel (EtOAc: *n*-hexane = 1 : 4): ^{1}H NMR (DMSO-d_6, 500 MHz) δ 13.35 (s, 1H, NH), 10.37 (s, 1H, NH), 8.05 (d, 2H, J = 8.1 Hz, Ar−H), 7.67 (d, 2H, J = 8.3 Hz, Ar−H), 7.31 (dd, 2H, J = 8.5, 5.6 Hz, Ar−H), 7.15 (t, 2H, J = 8.8 Hz, Ar−H), 6.56 (s, 1H, pyrazole−H), 4.03 (s, 2H, Ar−CH_2); ^{13}C NMR (DMSO-d_6, 100 MHz) δ 162.2, 161.0, 159.8, 146.7, 144.1, 142.6, 134.8, 130.4, 130.3, 125.8, 123.8, 123.5, 123.2, 123.1, 122.8, 120.0, 115.4, 115.2, 104.9, 30.1; LR-MS (ESI+) *m/z* 364 [M + H]$^+$; HR-MS (ESI+) calcd for $C_{18}H_{14}F_4N_3O$ [M + H]$^+$ 364.1068; found 364.1064.

*4.1.4.11. 3-(4-Fluorobenzyl)-N-(4-methoxyphenyl)-1H-pyrazole-5-carboxamide (**15**).* 3-(4-Fluorobenzyl)-1*H*-pyrazole-5-carboxylic acid (**5b**) (52.5 mg, 0.238 mmol) and 4-methoxyaniline (29.3 mg, 0.238 mmol) afforded 54.0 mg (70%) of **15** as white solid. **15** was purified by flash column chromatography on silica gel (EtOAc: *n*-hexane = 1 : 2 to 1 : 1): ^{1}H NMR (DMSO-d_6, 400 MHz) δ 13.25 (s, 1H, NH), 9.88 (s, 1H, NH), 7.69 (d, 2H, J = 8.8 Hz, Ar−H), 7.31 (m, 2H, Ar−H), 7.15 (m, 2H, Ar−H), 6.88 (d, 2H, J = 6.6 Hz, Ar−H), 6.49 (s, 1H, pyrazole−H), 4.01 (s, 2H, Ar−CH_2), 3.71 (s, 3H, OCH_3); ^{13}C NMR (DMSO-d_6, 100 MHz) δ 162.2, 160.2, 159.8, 155.3, 147.2, 143.9, 135.0, 134.9, 132.1, 130.4, 130.3, 121.7, 115.4, 115.2, 113.7, 104.6, 55.2, 30.1; LR-MS (ESI+) *m/z* 326 [M + H]$^+$; HR-MS (ESI+) calcd for $C_{18}H_{17}FN_3O_2$ [M + H]$^+$ 326.1299; found 326.1296.

*4.1.4.12. Methyl 4-(3-(4-fluorobenzyl)-1H-pyrazole-5-carboxamido) benzoate (**16**).* 3-(4-Fluorobenzyl)-1*H*-pyrazole-5-carboxylic acid (**5b**) (68.9 mg, 0.313 mmol) and methyl 4-aminobenzoate (47.3 mg, 0.313 mmol) afforded 44.2 mg (40%) of **16** as pale yellow solid. **16** was purified by flash column chromatography on silica gel (EtOAc: *n*-hexane = 1 : 2): ^{1}H NMR (DMSO-d_6, 400 MHz) δ 13.36 (s, 1H, NH), 10.36 (s, 1H, NH), 7.98 (d, 2H, J = 8.7 Hz, Ar−H), 7.91 (d, 2H, J = 8.4 Hz, Ar−H), 7.31 (dd, 2H, J = 8.4, 5.7 Hz, Ar−H), 7.15 (t, 2H, J = 8.8 Hz, Ar−H), 6.55 (s, 1H, pyrazole−H), 4.03 (s, 2H, Ar−CH_2), 3.82 (s, 3H, $COOCH_3$); ^{13}C NMR (DMSO-d_6, 100 MHz) δ 165.9, 162.2, 160.9, 159.8, 146.7, 144.1, 143.5, 134.8, 134.8, 130.4, 130.3, 130.0, 124.0, 119.4, 115.4, 115.2, 104.9, 51.9, 30.1; LR-MS (ESI+) *m/z* 354 [M + H]$^+$; HR-MS (ESI+) calcd for $C_{19}H_{17}FN_3O_3$ [M + H]$^+$ 354.1248; found 354.1263.

*4.1.4.13. N-(4-Fluorophenyl)-3-(4-methoxybenzyl)-1H-pyrazole-5-carboxamide (**17**).*
3-(4-Methoxybenzyl)-1*H*-pyrazole-5-carboxylic acid (**5c**) (100 mg, 0.431 mmol) and 4-fluoroaniline (40.8 μL, 0.431 mmol) afforded 71.5 mg (51%) of **17** as white solid. **17** was purified by flash column chromatography on silica gel (EtOAc: *n*-hexane = 1 : 2): ^{1}H NMR (DMSO-d_6, 400 MHz) δ 13.26 (s, 1H, NH), 10.10 (s, 1H, NH), 7.83 (m, 2H, Ar−H), 7.19 (d, 2H, J = 8.4 Hz, Ar−H), 7.15 (m, 2H, Ar−H), 6.88 (t, 2H, J = 8.9 Hz, Ar−H), 6.48 (s, 1H, pyrazole−H), 3.95 (s, 2H, Ar−CH_2), 3.72 (s, 3H, OCH_3); ^{13}C NMR (DMSO-d_6, 100 MHz) δ 160.4, 159.1, 157.7, 156.7, 146.7, 144.3, 135.2, 130.4, 129.3, 121.8, 121.7, 115.0, 114.8, 113.8, 104.4, 54.9, 29.9; LR-MS (ESI+) *m/z* 326 [M + H]$^+$; HR-MS (ESI+) calcd for $C_{18}H_{17}FN_3O_2$ [M + H]$^+$ 326.1299; found 326.1293.

*4.1.4.14. 3-(4-Methoxybenzyl)-N-phenyl-1H-pyrazole-5-carboxamide (**18**).*
3-(4-Methoxybenzyl)-1*H*-pyrazole-5-carboxylic acid (**5c**) (100 mg, 0.431 mmol) and aniline (39.3 μL, 0.431 mmol) afforded 58.3 mg (44%) of **18** as white solid. **18** was purified by flash column chromatography on silica gel (EtOAc: *n*-hexane = 1 : 2): ^{1}H NMR (DMSO-d_6, 400 MHz) δ 13.25 (s, 1H, NH), 9.96 (s, 1H, NH), 7.80 (d, 2H, J = 7.9 Hz, Ar−H), 7.30 (t, 2H, J = 7.4 Hz, Ar−H), 7.19 (d, 2H, J = 8.3 Hz, Ar−H), 7.05 (t, 1H, J = 7.0 Hz, Ar−H), 6.89 (d, 2H, J = 8.2 Hz, Ar−H), 6.48 (s, 1H, pyrazole−H), 3.95 (s, 2H, Ar−CH_2), 3.72 (s, 3H, OCH_3); ^{13}C NMR (DMSO-d_6, 100 MHz) δ 160.6, 157.9, 147.0, 144.6, 139.0, 130.6, 129.5, 128.6, 123.3, 120.1, 114.0, 104.5, 55.1, 30.1; LR-MS (ESI+) *m/z* 308 [M + H]$^+$; HR-MS (ESI+) calcd for $C_{18}H_{18}N_3O_2$ [M + H]$^+$ 308.1394; found 308.1384.

*4.1.4.15. N-(4-(tert-Butyl)phenyl)-3-(4-methoxybenzyl)-1H-pyrazole-5-carboxamide (**19**).*
3-(4-Methoxybenzyl)-1*H*-pyrazole-5-carboxylic acid (**5c**) (100 mg, 0.431 mmol) and 4-*t*-butylaniline (68.6 μL, 0.431 mmol) afforded 66.3 mg (42%) of **19** as pale yellow solid. **19** was purified by flash column chromatography on silica gel (EtOAc: *n*-hexane = 2 : 3): ^{1}H NMR ($CDCl_3$, 400 MHz) δ 8.67 (s, 1H, NH), 7.56 (d, 2H, J = 8.6 Hz, Ar−H), 7.34 (d, 2H, J = 8.6 Hz, Ar−H), 7.12 (d, 2H, J = 8.5 Hz, Ar−H), 6.84 (d, 2H, J = 8.5 Hz, Ar−H), 6.68 (s, 1H, pyrazole−H), 3.97 (s, 2H, Ar−CH_2), 3.77 (s, 3H, OCH_3), 1.30 (s, 9H, $(CH_3)_3$); ^{13}C NMR ($CDCl_3$, 100 MHz) δ 160.1, 158.7, 147.5, 147.2, 145.3, 135.2, 129.9, 129.1, 125.9, 119.7, 114.4, 105.3, 55.4, 34.5, 31.5, 31.1; LR-MS (ESI+) *m/z* 364 [M + H]$^+$; HR-MS (ESI+) calcd for $C_{22}H_{26}N_3O_2$ [M + H]$^+$ 364.2020; found 364.2023.

*4.1.4.16. 3-(4-Methoxybenzyl)-N-(4-(trifluoromethyl)phenyl)-1H-pyrazole-5-carboxamide (**20**).*
3-(4-Methoxybenzyl)-1*H*-pyrazole-5-carboxylic acid (**5c**) (56.3 mg, 0.242 mmol) and 4-(trifluoromethyl)aniline (30.4 μL, 0.242 mmol) afforded 30.9 mg (34%) of **20** as pale yellow solid. **20** was purified by flash column chromatography on silica gel (EtOAc: *n*-hexane = 1 : 4): ^{1}H NMR (DMSO-d_6, 500 MHz) δ 13.31 (s, 1H, NH), 10.36 (s, 1H, NH), 8.04 (d, 2H, J = 7.8 Hz, Ar−H), 7.67 (d, 2H, J = 8.4 Hz, Ar−H), 7.19 (d, 2H, J = 8.7 Hz, Ar−H), 6.89 (d, 2H, J = 8.7 Hz, Ar−H), 6.52 (s, 1H, pyrazole−H), 3.96 (s, 2H, Ar−CH_2), 3.72 (s, 3H, OCH_3); ^{13}C NMR (DMSO-d_6, 100 MHz) δ 161.0, 157.9, 146.6, 144.7, 142.6, 130.5, 129.5, 125.8, 125.8, 123.7, 123.4, 123.1, 122.8, 119.9, 113.9, 104.7, 55.0, 30.1; LR-MS (ESI+) *m/z* 376 [M + H]$^+$; HR-MS (ESI+) calcd for $C_{19}H_{17}F_3N_3O_2$ [M + H]$^+$ 376.1267; found 376.1284.

*4.1.4.17. 3-(4-Methoxybenzyl)-N-(4-methoxyphenyl)-1H-pyrazole-5-carboxamide (**21**).*

3-(4-Methoxybenzyl)-1*H*-pyrazole-5-carboxylic acid (**5c**) (100 mg, 0.431 mmol) and 4-methoxyaniline (53.1 mg, 0.431 mmol) afforded 60.7 mg (42%) of **21** as white solid. **21** was purified by flash column chromatography on silica gel (EtOAc: *n*-hexane = 1 : 1): ^{1}H NMR ($CDCl_3$, 400 MHz) δ 10.59 (brs, 1H, NH), 8.62 (s, 1H, NH), 7.53 (d, 2H, J = 8.8 Hz, Ar−H), 7.11 (d, 2H, J = 8.4 Hz, Ar−H), 6.86 (d, 2H, J = 9.0 Hz, Ar−H), 6.84 (d, 2H, J = 8.6 Hz, Ar−H), 6.66 (s, 1H, pyrazole−H), 3.96 (s, 2H, Ar−CH_2), 3.78 (s, 3H, OCH_3), 3.77 (s, 3H, OCH_3); ^{13}C NMR ($CDCl_3$, 100 MHz) δ 160.0, 158.7, 156.4, 147.3, 145.4, 130.9, 129.8, 129.2, 121.8, 114.4, 114.3, 105.2, 55.6, 55.4, 31.4; LR-MS (ESI+) m/z 338 $[M + H]^+$; HR-MS (ESI+) calcd for $C_{19}H_{20}N_3O_3$ $[M + H]^+$ 338.1499; found 338.1502.

*4.1.4.18. Methyl 4-(3-(4-methoxybenzyl)-1H-pyrazole-5-carboxamido)benzoate (**22**).*

3-(4-Methoxybenzyl)-1*H*-pyrazole-5-carboxylic acid (**5c**) (57.5 mg, 0.248 mmol) and methyl 4-aminobenzoate (37.5 mg, 0.248 mmol) afforded 20.3 mg (22%) of **22** as pale yellow solid. **22** was purified by flash column chromatography on silica gel (EtOAc: *n*-hexane = 1 : 2): ^{1}H NMR (DMSO-d_6, 400 MHz) δ 13.32 (s, 1H, NH), 10.34 (s, 1H, NH), 7.97 (d, 2H, J = 8.8 Hz, Ar−H), 7.91 (d, 2H, J = 8.6 Hz, Ar−H), 7.19 (d, 2H, J = 8.6 Hz, Ar−H), 6.89 (d, 2H, J = 8.6 Hz, Ar−H), 6.51 (s, 1H, pyrazole−H), 3.96 (s, 2H, Ar−CH_2), 3.82 (s, 3H, $COOCH_3$), 3.72 (s, 3H, OCH_3); ^{13}C NMR (DMSO-d_6, 100 MHz) δ 165.9, 160.9, 157.9, 146.6, 144.7, 143.5, 130.5, 130.0, 129.5, 123.9, 119.4, 114.0, 104.7, 55.1, 51.9, 30.1; LR-MS (ESI+) m/z 366 $[M + H]^+$; HR-MS (ESI+) calcd for $C_{20}H_{20}N_3O_4$ $[M + H]^+$ 366.1448; found 366.1458.

*4.1.4.19. 3-(4-Chlorobenzyl)-N-(2-methoxyphenyl)-1H-pyrazole-5-carboxamide (**23**).*

3-(4-Chlorobenzyl)-1*H*-pyrazole-5-carboxylic acid (**5a**) (45.5 mg, 0.192 mmol) and 2-methoxyaniline (21.7 μL, 0.192 mmol) afforded 20.2 mg (31%) of **23** as pale yellow solid. **23** was purified by flash column chromatography on silica gel (EtOAc: *n*-hexane = 1 : 4 to 1 : 1): ^{1}H NMR (DMSO-d_6, 400 MHz) δ 13.33 (s, 1H, NH), 9.31 (s, 1H, NH), 8.28 (d, 1H, J = 7.9 Hz, Ar−H), 7.38 (d, 2H, J = 7.1 Hz, Ar−H), 7.29 (d, 2H, J = 7.3 Hz, Ar−H), 7.08 (m, 2H, Ar−H), 6.95 (t, 1H, J = 6.8 Hz, Ar−H), 6.53 (s, 1H, pyrazole−H), 4.03 (s, 2H, Ar−CH_2), 3.89 (s, 3H, OCH_3); ^{13}C NMR (DMSO-d_6, 100 MHz) δ 159.5, 148.1, 146.7, 144.2, 137.6, 131.2, 130.4, 128.6, 127.2, 123.8, 120.7, 119.0, 110.9, 104.5, 56.0, 30.3; LR-MS (ESI+) m/z 342 $[M + H]^+$; HR-MS (ESI+) calcd for $C_{18}H_{17}ClN_3O_2$ $[M + H]^+$ 342.1004; found 342.1006.

*4.1.4.20. 3-(4-Chlorobenzyl)-N-(3-methoxyphenyl)-1H-pyrazole-5-carboxamide (**24**).*

3-(4-Chlorobenzyl)-1*H*-pyrazole-5-carboxylic acid (**5a**) (45.3 mg, 0.191 mmol) and 3-methoxyaniline (21.5 μL, 0.191 mmol) afforded 30.3 mg (46%) of **24** as a brown oil. **24** was purified by flash column chromatography on silica gel (EtOAc: *n*-hexane = 1 : 2 to 1 : 1): ^{1}H NMR (DMSO-d_6, 400 MHz) δ 13.28 (s, 1H, NH), 9.92 (s, 1H, NH), 7.49 (s, 1H, Ar−H), 7.40 (s, 1H, Ar−H), 7.38 (d, 2H, J = 7.4 Hz, Ar−H), 7.30 (d, 2H, J = 8.4 Hz, Ar−H), 7.20 (t, 1H, J = 8.1 Hz, Ar−H), 6.64 (d, 1H, J = 7.4 Hz, Ar−H), 6.52 (s, 1H, pyrazole−H), 4.03 (s, 2H, Ar−CH_2), 3.73 (s, 3H, OCH_3); ^{13}C NMR (DMSO-d_6, 100 MHz) δ 160.6, 159.5, 147.1, 143.6, 140.1, 137.7, 131.2, 130.4, 129.4, 128.6, 112.4, 108.9, 105.9, 104.8, 55.0, 30.3; LR-MS (ESI+) m/z 342 $[M + H]^+$; HR-MS (ESI+) calcd for $C_{18}H_{17}ClN_3O_2$ $[M + H]^+$ 342.1004; found 342.1001.

*4.1.4.21. 3-(4-Chlorobenzyl)-N-(2,3-dimethoxyphenyl)-1H-pyrazole-5-carboxamide (**25**).*

3-(4-Chlorobenzyl)-1*H*-pyrazole-5-carboxylic acid (**5a**) (45.1 mg, 0.190 mmol) and 2,3-dimethoxyaniline (30.1 μL, 0.224 mmol) afforded 20.7 mg (25%) of **25** as white solid. **25** was purified by flash column chromatography on silica gel (EtOAc: *n*-hexane = 1 : 3): ^{1}H NMR (DMSO-d_6, 400 MHz) δ 13.34 (s, 1H, NH), 9.38 (s, 1H, NH), 7.92 (d, 1H, J = 8.2 Hz, Ar−H), 7.38 (d, 2H, J = 8.4 Hz, Ar−H), 7.29 (d, 2H, J = 8.3 Hz, Ar−H), 7.05 (t, 1H, J = 8.3 Hz, Ar−H), 6.81 (d, 1H, J = 8.6 Hz, Ar−H), 6.54 (s, 1H, pyrazole−H), 4.03 (s, 2H, Ar−CH_2), 3.82 (s, 3H, OCH_3), 3.80 (s, 3H, OCH_3); ^{13}C NMR (DMSO-d_6, 100 MHz) δ 159.5, 152.0, 146.7, 144.2, 137.6, 137.3, 131.8, 131.2, 130.4, 128.6, 124.1, 111.7, 107.9, 104.5, 60.4, 55.8, 30.2; LR-MS (ESI+) m/z 372 $[M + H]^+$; HR-MS (ESI+) calcd for $C_{19}H_{19}ClN_3O_3$ $[M + H]^+$ 372.1109; found 372.1110.

*4.1.4.22. 3-(4-Chlorobenzyl)-N-(2,4-dimethoxyphenyl)-1H-pyrazole-5-carboxamide (**26**).*

3-(4-Chlorobenzyl)-1*H*-pyrazole-5-carboxylic acid (**5a**) (599 mg, 2.53 mmol) and 2,4-dimethoxyaniline (433 μL, 3.04 mmol) afforded 514 mg (55%) of **26** as brown solid. **26** was purified by flash column chromatography on silica gel (EtOAc: *n*-hexane = 1 : 4): ^{1}H NMR ($CDCl_3$, 400 MHz) δ 9.01 (s, 1H, NH), 8.31 (d, 1H, J = 8.4 Hz, Ar−H), 7.22 (d, 2H, J = 8.3 Hz, Ar−H), 7.08 (d, 2H, J = 8.4 Hz, Ar−H), 6.61 (s, 1H, pyrazole−H), 6.48 (s, 1H, Ar−H), 6.46 (d, 1H, J = 2.6 Hz, Ar−H), 3.97 (s, 2H, Ar−CH_2), 3.82 (s, 3H, OCH_3), 3.79 (s, 3H, OCH_3); ^{13}C NMR ($CDCl_3$, 100 MHz) δ 160.0, 157.0, 150.2, 147.5, 145.0, 136.4, 133.2, 130.3, 129.3, 121.3, 121.2, 105.5, 104.2, 99.1, 56.2, 56.0, 32.0; LR-MS (ESI+) m/z 372 $[M + H]^+$; HR-MS (ESI+) calcd for $C_{19}H_{19}ClN_3O_3$ $[M + H]^+$ 372.1109; found 372.1114.

*4.1.4.23. 3-(4-Chlorobenzyl)-N-(2,5-dimethoxyphenyl)-1H-pyrazole-5-carboxamide (**27**).*

3-(4-Chlorobenzyl)-1*H*-pyrazole-5-carboxylic acid (**5a**) (613 mg, 2.59 mmol) and 2,5-dimethoxyaniline (476 mg, 3.11 mmol) afforded 422 mg (44%) of **27** as pale yellow solid. **27** was purified by flash column chromatography on silica gel (EtOAc: *n*-hexane = 1 : 4): ^{1}H NMR ($CDCl_3$, 400 MHz) δ 9.22 (s, 1H, NH), 8.24 (d, 1H, J = 2.8 Hz, Ar−H), 7.28 (d, 2H, J = 8.4 Hz, Ar−H), 7.14 (d, 2H, J = 8.2 Hz, Ar−H), 6.81 (d, 1H, J = 9.0 Hz, Ar−H), 6.66 (s, 1H, pyrazole−H), 6.59 (dd, 1H, J = 8.9, 3.0 Hz, Ar−H), 4.03 (s, 2H, Ar−CH_2), 3.86 (s, 3H, OCH_3), 3.80 (s, 3H, OCH_3); ^{13}C NMR ($CDCl_3$, 100 MHz) δ 159.8, 153.9, 147.4, 144.6, 142.6, 135.7, 133.1, 130.1, 129.1, 128.2, 111.0, 108.8, 106.1, 105.3, 56.5, 55.9, 31.7; LR-MS (ESI+) m/z 372 $[M + H]^+$; HR-MS (ESI+) calcd for $C_{19}H_{19}ClN_3O_3$ $[M + H]^+$ 372.1109; found 372.1111.

*4.1.4.24. N-(Benzo[d][1,3]dioxol-5-yl)-3-(4-chlorobenzyl)-1H-pyrazole-5-carboxamide (**28**).*

3-(4-Chlorobenzyl)-1*H*-pyrazole-5-carboxylic acid (**5a**) (48.8 mg, 0.206 mmol) and 3,4-(methylenedioxy)aniline (28.3 mg, 0.206 mmol) afforded 33.6 mg (46%) of **28** as pale yellow solid. **28** was purified by flash column chromatography on silica gel (EtOAc: *n*-hexane = 1 : 3): ^{1}H NMR (DMSO-d_6, 400 MHz) δ 13.26 (s, 1H, NH), 9.92 (s, 1H, NH), 7.45 (s, 1H, Ar−H), 7.38 (d, 2H, J = 7.8 Hz, Ar−H), 7.28 (d, 2H, J = 8.2 Hz, Ar−H), 7.26 (m, 1H, Ar−H), 6.85 (d, 1H, J = 7.8 Hz, Ar−H), 6.49 (s, 1H, pyrazole−H), 5.98 (s, 2H, OCH_2O), 4.02 (s, 2H, Ar−CH_2); ^{13}C NMR (DMSO-d_6, 100 MHz) δ 160.2, 147.1, 146.9, 143.5, 143.0, 137.7, 133.3, 131.2, 130.4, 128.5, 113.1, 107.9, 104.7, 102.3, 100.9, 30.2; LR-MS (ESI+) m/z 356 $[M + H]^+$; HR-MS (ESI+) calcd for $C_{18}H_{15}ClN_3O_3$ $[M + H]^+$ 356.0796; found 356.0806.

*4.1.4.25. 3-(4-Fluorobenzyl)-N-(2-methoxyphenyl)-1H-pyrazole-5-carboxamide (**29**).* 3-(4-Fluorobenzyl)-1*H*-pyrazole-5-carboxylic acid (**5b**) (78.2 mg, 0.355 mmol) and 2-methoxyaniline (40.0 μL, 0.355 mmol) afforded 61.7 mg (53%) of **29** as pale yellow solid. **29** was purified by flash column chromatography on silica gel (EtOAc: *n*-hexane = 1 : 2 to 1 : 1): ^{1}H NMR (DMSO-d_6, 400 MHz) δ 13.31 (s, 1H, NH), 9.32 (s, 1H, NH), 8.30 (d, 1H, J = 7.6 Hz, Ar−H), 7.31 (dd, 2H, J = 8.4, 5.6 Hz, Ar−H), 7.15 (t, 2H, J = 8.9 Hz, Ar−H), 7.08 (m, 1H, Ar−H), 7.06 (m, 1H, Ar−H), 6.95 (m, 1H, Ar−H), 6.53 (s, 1H,

pyrazole−H), 4.03 (s, 2H, Ar−CH_2), 3.89 (s, 3H, OCH_3); ^{13}C NMR (DMSO-d_6, 100 MHz) δ 162.2, 159.8, 159.5, 148.1, 146.7, 144.6, 134.7, 134.7, 130.4, 130.3, 127.2, 123.7, 120.7, 119.0, 115.4, 115.2, 110.9, 104.4, 56.0, 30.1; LR-MS (ESI+) *m/z* 326 $[M + H]^+$; HR-MS (ESI+) calcd for $C_{18}H_{17}FN_3O_2$ $[M + H]^+$ 326.1299; found 326.1295.

*4.1.4.26. 3-(4-Fluorobenzyl)-N-(3-methoxyphenyl)-1H-pyrazole-5-carboxamide (**30**).* 3-(4-Fluorobenzyl)-1*H*-pyrazole-5-carboxylic acid (**5b**) (53.3 mg, 0.242 mmol) and 3-methoxyaniline (27.2 μL, 0.242 mmol) afforded 39.9 mg (51%) of **30** as pale yellow solid. **30** was purified by flash column chromatography on silica gel (EtOAc: *n*-hexane = 1 : 2 to 1 : 1): ^{1}H NMR (DMSO-d_6, 400 MHz) δ 13.27 (s, 1H, NH), 9.92 (s, 1H, NH), 7.50 (s, 1H, Ar−H), 7.41 (d, 1H, *J* = 8.3 Hz, Ar−H), 7.31 (dd, 2H, *J* = 8.3, 5.6 Hz, Ar−H), 7.21 (d, 1H, *J* = 8.2 Hz, Ar−H), 7.15 (t, 2H, *J* = 8.9 Hz, Ar−H), 6.63 (dd, 1H, *J* = 8.2, 2.1 Hz, Ar−H), 6.51 (s, 1H, pyrazole−H), 4.02 (s, 2H, Ar−CH_2), 3.73 (s, 3H, OCH_3); ^{13}C NMR (DMSO-d_6, 100 MHz) δ 162.2, 160.5, 159.8, 159.4, 147.1, 144.0, 140.1, 134.9, 134.8, 130.4, 130.3, 129.3, 115.4, 115.2, 112.3, 108.8, 105.9, 104.7, 55.0, 30.1; LR-MS (ESI+) *m/z* 326 $[M + H]^+$; HR-MS (ESI+) calcd for $C_{18}H_{17}FN_3O_2$ $[M + H]^+$ 326.1299; found 326.1301.

*4.1.4.27. N-(2,3-Dimethoxyphenyl)-3-(4-fluorobenzyl)-1H-pyrazole-5-carboxamide (**31**).*
3-(4-Fluorobenzyl)-1*H*-pyrazole-5-carboxylic acid (**5b**) (67.9 mg, 0.308 mmol) and 2,3-dimethoxyaniline (41.4 μL, 0.308 mmol) afforded 58.4 mg (52%) of **31** as pale yellow solid. **31** was purified by flash column chromatography on silica gel (EtOAc: *n*-hexane = 1 : 3): ^{1}H NMR (DMSO-d_6, 400 MHz) δ 13.37 (s, 1H, NH), 9.40 (s, 1H, NH), 7.94 (d, 1H, *J* = 8.2 Hz, Ar−H), 7.31 (m, 2H, Ar−H), 7.15 (t, 2H, *J* = 8.8 Hz, Ar−H), 7.06 (t, 1H, *J* = 8.3 Hz, Ar−H), 6.81 (d, 1H, *J* = 8.4 Hz, Ar−H), 6.54 (s, 1H, pyrazole−H), 4.03 (s, 2H, Ar−CH_2), 3.82 (s, 3H, OCH_3), 3.81 (s, 3H, OCH_3); ^{13}C NMR (DMSO-d_6, 100 MHz) δ 162.2, 159.8, 159.6, 152.0, 146.7, 144.7, 137.3, 134.7, 134.7, 131.8, 130.4, 130.3, 124.1, 115.5, 115.2, 111.7, 107.9, 104.4, 60.4, 55.8, 30.1; LR-MS (ESI+) *m/z* 356 $[M + H]^+$; HR-MS (ESI+) calcd for $C_{19}H_{19}FN_3O_3$ $[M + H]^+$ 356.1405; found 356.1419.

*4.1.4.28. N-(2,4-Dimethoxyphenyl)-3-(4-fluorobenzyl)-1H-pyrazole-5-carboxamide (**32**).*
3-(4-Fluorobenzyl)-1*H*-pyrazole-5-carboxylic acid (**5b**) (70.6 mg, 0.321 mmol) and 2,4-dimethoxyaniline (45.7 μL, 0.321 mmol) afforded 24.9 mg (22%) of **32** as a light brown oil. **32** was purified by flash column chromatography on silica gel (EtOAc: *n*-hexane = 1 : 2 to 1 : 1): ^{1}H NMR ($CDCl_3$, 400 MHz) δ 10.88 (brs, 1H, NH), 9.03 (s, 1H, NH), 8.33 (d, 1H, *J* = 7.6 Hz, Ar−H), 7.13 (m, 2H, Ar−H), 6.95 (t, 2H, *J* = 8.6 Hz, Ar−H), 6.63 (s, 1H, pyrazole−H), 6.49 (s, 1H, Ar−H), 6.47 (m, 1H, Ar−H), 3.99 (s, 2H, Ar−CH_2), 3.83 (s, 3H, OCH_3), 3.79 (s, 3H, OCH_3); ^{13}C NMR ($CDCl_3$, 100 MHz) δ 163.1, 160.7, 159.6, 156.6, 149.8, 147.3, 145.0, 133.2, 133.1, 130.3, 130.2, 121.0, 120.8, 115.9, 115.7, 105.1, 103.8, 98.8, 55.9, 55.7, 31.5; LR-MS (ESI+) *m/z* 356 $[M + H]^+$; HR-MS (ESI+) calcd for $C_{19}H_{19}FN_3O_3$ $[M + H]^+$ 356.1405; found 356.1405.

*4.1.4.29. N-(2,5-Dimethoxyphenyl)-3-(4-fluorobenzyl)-1H-pyrazole-5-carboxamide (**33**).*
3-(4-Fluorobenzyl)-1*H*-pyrazole-5-carboxylic acid (**5b**) (74.6 mg, 0.339 mmol) and 2,5-dimethoxyaniline (52.0 mg, 0.339 mmol) afforded 11.0 mg (9%) of **33** as a brown oil. **33** was purified by flash column chromatography on silica gel (EtOAc: *n*-hexane = 1 : 2 to 1 : 1): ^{1}H NMR ($CDCl_3$, 400 MHz) δ 9.25 (s, 1H, NH), 8.24 (d, 1H, *J* = 2.7 Hz, Ar−H), 7.17 (dd, 2H, *J* = 7.9, 5.6 Hz, Ar−H), 7.00 (t, 2H, *J* = 8.2 Hz, Ar−H), 6.81 (d, 1H, *J* = 8.8 Hz, Ar−H), 6.67 (s, 1H, pyrazole−H), 6.59 (dd, 1H, *J* = 8.8, 2.4 Hz, Ar−H), 4.03 (s, 2H, Ar−CH_2), 3.86 (s, 3H, OCH_3), 3.80 (s, 3H, OCH_3); ^{13}C NMR ($CDCl_3$, 100 MHz) δ 163.2, 160.8, 159.8, 153.9, 147.6, 144.9, 142.6, 132.9, 132.8, 130.3, 130.3, 128.3, 116.0, 115.8, 110.9, 108.8, 106.0, 105.3, 56.5, 55.9, 31.6; LR-MS (ESI+) *m/z* 356 $[M + H]^+$; HR-MS (ESI+) calcd for $C_{19}H_{19}FN_3O_3$ $[M + H]^+$ 356.1405; found 356.1413.

*4.1.4.30. N-(Benzo[d][1,3]dioxol-5-yl)-3-(4-fluorobenzyl)-1H-pyrazole-5-carboxamide (**34**).*
3-(4-Fluorobenzyl)-1*H*-pyrazole-5-carboxylic acid (**5b**) (78.0 mg, 0.354 mmol) and 3,4-(methylenedioxy)aniline (48.5 mg, 0.354 mmol) afforded 61.5 mg (51%) of **34** as brown solid. **34** was purified by flash column chromatography on silica gel (EtOAc: *n*-hexane = 1 : 2): ^{1}H NMR (DMSO-d_6, 400 MHz) δ 13.25 (s, 1H, NH), 9.91 (s, 1H, NH), 7.46 (s, 1H, Ar−H), 7.30 (m, 2H, Ar−H), 7.26 (d, 1H, *J* = 8.6 Hz, Ar−H), 7.15 (t, 2H, *J* = 8.7 Hz, Ar−H), 6.85 (d, 1H, *J* = 8.4 Hz, Ar−H), 6.49 (s, 1H, pyrazole−H), 5.98 (s, 2H, OCH_2O), 4.01 (s, 2H, Ar−CH_2); ^{13}C NMR (DMSO-d_6, 100 MHz) δ 162.2, 160.3, 159.8, 147.1, 146.9, 143.9, 143.0, 134.9, 134.9, 133.3, 130.4, 130.3, 115.4, 115.2, 113.1, 107.9, 104.6, 102.3, 100.9, 30.1; LR-MS (ESI+) *m/z* 340 $[M + H]^+$; HR-MS (ESI+) calcd for $C_{18}H_{15}FN_3O_3$ $[M + H]^+$ 340.1092; found 340.1105.

*4.1.4.31. 3-(4-Methoxybenzyl)-N-(2-methoxyphenyl)-1H-pyrazole-5-carboxamide (**35**).*
3-(4-Methoxybenzyl)-1*H*-pyrazole-5-carboxylic acid (**5c**) (70.1 mg, 0.302 mmol) and 2-methoxyaniline (34.1 μL, 0.302 mmol) afforded 44.9 mg (44%) of **35** as pale yellow solid. **35** was purified by flash column chromatography on silica gel (EtOAc: *n*-hexane = 1 : 4): ^{1}H NMR (DMSO-d_6, 400 MHz) δ 13.29 (s, 1H, NH), 9.32 (s, 1H, NH), 8.31 (d, 1H, *J* = 8.4 Hz, Ar−H), 7.18 (d, 2H, *J* = 7.0 Hz, Ar−H), 7.07 (m, 1H, Ar−H), 7.05 (m, 1H, Ar−H), 6.95 (t, 1H, *J* = 7.1 Hz, Ar−H), 6.88 (d, 2H, *J* = 6.9 Hz, Ar−H), 6.49 (s, 1H, pyrazole−H), 3.95 (s, 2H, Ar−CH_2), 3.89 (s, 3H, OCH_3), 3.72 (s, 3H, OCH_3); ^{13}C NMR (DMSO-d_6, 100 MHz) δ 159.6, 158.0, 148.0, 146.6, 145.2, 130.4, 129.5, 127.2, 123.7, 120.7, 118.9, 114.0, 110.9, 104.2, 56.0, 55.1, 30.1; LR-MS (ESI+) *m/z* 338 $[M + H]^+$; HR-MS (ESI+) calcd for $C_{19}H_{20}N_3O_3$ $[M + H]^+$ 338.1499; found 338.1513.

*4.1.4.32. 3-(4-Methoxybenzyl)-N-(3-methoxyphenyl)-1H-pyrazole-5-carboxamide (**36**).*
3-(4-Methoxybenzyl)-1*H*-pyrazole-5-carboxylic acid (**5c**) (70.3 mg, 0.303 mmol) and 3-methoxyaniline (34.0 μL, 0.303 mmol) afforded 59.3 mg (58%) of **36** as pale yellow solid. **36** was purified by flash column chromatography on silica gel (EtOAc: *n*-hexane = 1 : 4): ^{1}H NMR ($CDCl_3$, 400 MHz) δ 8.76 (s, 1H, NH), 7.43 (s, 1H, Ar−H), 7.21 (t, 1H, *J* = 8.1 Hz, Ar−H), 7.09 (m, 3H, Ar−H), 6.82 (d, 2H, *J* = 7.8 Hz, Ar−H), 6.66 (m, 1H, Ar−H), 6.65 (s, 1H, pyrazole−H), 3.95 (s, 2H, Ar−CH_2), 3.77 (s, 3H, OCH_3), 3.75 (s, 3H, OCH_3); ^{13}C NMR (DMSO-d_6, 100 MHz) δ 160.6, 159.4, 157.9, 147.0, 144.6, 140.1, 130.6, 129.5, 129.4, 114.0, 112.4, 108.8, 105.9, 104.5, 55.1, 55.0, 30.1; LR-MS (ESI+) *m/z* 338 $[M + H]^+$; HR-MS (ESI+) calcd for $C_{19}H_{20}N_3O_3$ $[M + H]^+$ 338.1499; found 338.1512.

*4.1.4.33. N-(2,3-Dimethoxyphenyl)-3-(4-methoxybenzyl)-1H-pyrazole-5-carboxamide (**37**).*
3-(4-Methoxybenzyl)-1*H*-pyrazole-5-carboxylic acid (**5c**) (70.0 mg, 0.301 mmol) and 2,3-dimethoxyaniline (40.4 μL, 0.301 mmol) afforded 43.3 mg (39%) of **37** as a yellow oil. **37** was purified by flash column chromatography on silica gel (EtOAc: *n*-hexane = 1 : 4): ^{1}H NMR (DMSO-d_6, 400 MHz) δ 13.33 (s, 1H, NH), 9.39 (s, 1H, NH), 7.93 (d, 1H, *J* = 8.2 Hz, Ar−H), 7.19 (d, 2H, *J* = 8.5 Hz, Ar−H), 7.05 (t, 1H, *J* = 8.4 Hz, Ar−H), 6.88 (d, 2H, *J* = 8.3 Hz, Ar−H), 6.81 (d, 1H, *J* = 8.4 Hz, Ar−H), 6.49 (s, 1H, pyrazole−H), 3.95 (s, 2H, Ar−CH_2), 3.82 (s, 3H, OCH_3), 3.80 (s, 3H, OCH_3), 3.71 (s, 3H, OCH_3); ^{13}C NMR (DMSO-d_6, 100 MHz) δ 159.6, 157.9, 152.0, 146.6, 145.3, 137.3, 131.9, 130.4, 129.5, 124.1, 114.0, 111.7, 107.9, 104.2, 60.4, 55.8, 55.1, 30.1; LR-MS (ESI+) *m/z* 368 $[M + H]^+$; HR-MS (ESI+) calcd for $C_{20}H_{22}N_3O_4$

$[M + H]^+$ 368.1605; found 368.1618.

*4.1.4.34. N-(2,4-Dimethoxyphenyl)-3-(4-methoxybenzyl)-1H-pyrazole-5-carboxamide (**38**).*

3-(4-Methoxybenzyl)-1*H*-pyrazole-5-carboxylic acid (**5c**) (100 mg, 0.431 mmol) and 2,4-dimethoxyaniline (66.0 mg, 0.431 mmol) afforded 48.3 mg (31%) of **38** as a dark brown oil. **38** was purified by flash column chromatography on silica gel (EtOAc: *n*-hexane = 1 : 1): ^{1}H NMR ($CDCl_3$, 400 MHz) δ 9.04 (s, 1H, NH), 8.36 (d, 1H, J = 9.5 Hz, Ar−H), 7.10 (d, 2H, J = 8.5 Hz, Ar−H), 6.82 (d, 2H, J = 8.6 Hz, Ar−H), 6.65 (s, 1H, pyrazole−H), 6.49 (m, 1H, Ar−H), 6.48 (m, 1H, Ar−H), 3.97 (s, 2H, Ar−CH_2), 3.83 (s, 3H, OCH_3), 3.79 (s, 3H, OCH_3), 3.77 (s, 3H, OCH_3); ^{13}C NMR ($CDCl_3$, 100 MHz) δ 159.7, 158.7, 156.5, 149.8, 147.6, 145.4, 129.8, 129.3, 121.2, 120.8, 114.4, 105.0, 103.8, 98.8, 55.9, 55.7, 55.4, 31.4; LR-MS (ESI+) m/z 368 $[M + H]^+$; HR-MS (ESI+) calcd for $C_{20}H_{22}N_3O_4$ $[M + H]^+$ 368.1605; found 368.1608.

*4.1.4.35. N-(2,5-Dimethoxyphenyl)-3-(4-methoxybenzyl)-1H-pyrazole-5-carboxamide (**39**).*

3-(4-Methoxybenzyl)-1*H*-pyrazole-5-carboxylic acid (**5c**) (104 mg, 0.448 mmol) and 2,5-dimethoxyaniline (68.6 mg, 0.448 mmol) afforded 13.9 mg (8%) of **39** as a brown oil. **39** was purified by flash column chromatography on silica gel (EtOAc: *n*-hexane = 2 : 3): ^{1}H NMR ($CDCl_3$, 400 MHz) δ 9.27 (s, 1H, NH), 8.26 (d, 1H, J = 3.0 Hz, Ar−H), 7.14 (d, 2H, J = 8.4 Hz, Ar−H), 6.87 (d, 2H, J = 8.6 Hz, Ar−H), 6.81 (d, 1H, J = 8.8 Hz, Ar−H), 6.69 (s, 1H, pyrazole−H), 6.59 (dd, 1H, J = 8.8, 3.1 Hz, Ar−H), 4.01 (s, 2H, Ar−CH_2), 3.86 (s, 3H, OCH_3), 3.81 (s, 3H, OCH_3), 3.80 (s, 3H, OCH_3); ^{13}C NMR ($CDCl_3$, 100 MHz) δ 159.9, 158.9, 154.0, 147.9, 145.3, 142.6, 129.9, 128.9, 128.4, 114.5, 111.0, 108.8, 105.9, 105.1, 56.5, 55.9, 55.5, 31.5; LR-MS (ESI+) m/z 368 $[M + H]^+$; HR-MS (ESI+) calcd for $C_{20}H_{22}N_3O_4$ $[M + H]^+$ 368.1605; found 368.1598.

*4.1.4.36. N-(Benzo[d][1,3]dioxol-5-yl)-3-(4-methoxybenzyl)-1H-pyrazole-5-carboxamide (**40**).*

3-(4-Methoxybenzyl)-1*H*-pyrazole-5-carboxylic acid (**5c**) (63.7 mg, 0.274 mmol) and 3,4-(methylenedioxy)aniline (37.6 mg, 0.274 mmol) afforded 44.6 mg (46%) of **40** as brown solid. **40** was purified by flash column chromatography on silica gel (EtOAc: *n*-hexane = 1 : 3): ^{1}H NMR (DMSO-d_6, 400 MHz) δ 13.21 (s, 1H, NH), 9.90 (s, 1H, NH), 7.46 (s, 1H, Ar−H), 7.26 (d, 1H, J = 7.4 Hz, Ar−H), 7.18 (d, 2H, J = 8.5 Hz, Ar−H), 6.88 (d, 2H, J = 8.6 Hz, Ar−H), 6.86 (m, 1H, Ar−H), 6.45 (s, 1H, pyrazole−H), 5.98 (s, 2H, OCH_2O), 3.94 (s, 2H, Ar−CH_2), 3.72 (s, 3H, OCH_3); ^{13}C NMR (DMSO-d_6, 100 MHz) δ 160.3, 157.9, 147.0, 146.9, 144.5, 143.0, 133.3, 130.6, 129.5, 113.9, 113.0, 107.9, 104.4, 102.3, 100.9, 55.1, 30.1; LR-MS (ESI+) m/z 352 $[M + H]^+$; HR-MS (ESI+) calcd for $C_{19}H_{18}N_3O_4$ $[M + H]^+$ 352.1292; found 352.1304.

*4.1.4.37. 3-(3-Chlorobenzyl)-N-(2,4-dimethoxyphenyl)-1H-pyrazole-5-carboxamide (**41**).*

3-(3-Chlorobenzyl)-1*H*-pyrazole-5-carboxylic acid (**5d**) (61.8 mg, 0.261 mmol) afforded 90.3 mg (93%) of **41** as brown solid. **41** was purified by flash column chromatography on silica gel (EtOAc: *n*-hexane = 1 : 2): ^{1}H NMR (DMSO-d_6, 400 MHz) δ 13.29 (s, 1H, NH), 9.12 (s, 1H, NH), 8.13 (d, 1H, J = 8.6 Hz, Ar−H), 7.34 (m, 2H, Ar−H), 7.30 (d, 1H, J = 7.6 Hz, Ar−H), 7.23 (d, 1H, J = 7.2 Hz, Ar−H), 6.67 (s, 1H, pyrazole−H), 6.55 (s, 1H, Ar−H), 6.52 (m, 1H, Ar−H), 4.05 (s, 2H, Ar−CH_2), 3.87 (s, 3H, OCH_3), 3.75 (s, 3H, OCH_3); ^{13}C NMR (DMSO-d_6, 100 MHz) δ 159.2, 156.1, 149.7, 146.9, 143.7, 141.1, 133.2, 130.5, 128.3, 127.2, 126.6, 120.5, 120.4, 104.5, 104.2, 98.8, 56.0, 55.3, 30.5; LR-MS (ESI+) m/z 372 $[M + H]^+$; HR-MS (ESI+) calcd for $C_{19}H_{19}ClN_3O_3$ $[M + H]^+$ 372.1109; found 372.1118.

*4.1.4.38. 3-(2-chlorobenzyl)-N-(2,4-dimethoxyphenyl)-1H-pyrazole-5-carboxamide (**42**).*

3-(2-Chlorobenzyl)-1*H*-pyrazole-5-carboxylic acid (**5e**) (71.6 mg, 0.303 mmol) afforded 67.4 mg (60%) of **42** as ivory solid. **42** was purified by flash column chromatography on silica gel (EtOAc: *n*-hexane = 1 : 2): ^{1}H NMR (DMSO-d_6, 400 MHz) δ 13.32 (s, 1H, NH), 9.13 (s, 1H, NH), 8.11 (d, 1H, J = 8.1 Hz, Ar−H), 7.47 (d, 1H, J = 6.6 Hz, Ar−H), 7.32 (m, 3H, Ar−H), 6.67 (s, 1H, pyrazole−H), 6.53 (d, 1H, J = 8.8 Hz, Ar−H), 6.41 (s, 1H, Ar−H), 4.14 (s, 2H, Ar−CH_2), 3.87 (s, 3H, OCH_3), 3.75 (s, 3H, OCH_3); ^{13}C NMR (DMSO-d_6, 100 MHz) δ 159.2, 156.2, 149.7, 146.9, 142.8, 136.0, 133.0, 130.8, 129.5, 128.8, 127.6, 120.5, 120.4, 104.5, 104.2, 98.9, 56.0, 55.4, 29.0; LR-MS (ESI+) m/z 372 $[M + H]^+$; HR-MS (ESI+) calcd for $C_{19}H_{19}ClN_3O_3$ $[M + H]^+$ 372.1109; found 372.1107.

*4.1.5. General procedures for the preparation of **43** and **46***

To a stirred solution of carboxylic acid in CH_2Cl_2 were added oxalyl chloride (3.0 equiv.) and 2 drops of DMF at ambient temperature. After stirring for 30 min, the reaction mixture was concentrated in vacuo and then diluted with CH_2Cl_2. To the reaction mixture were added aniline (1.0 equiv.) and triethylamine (2.0 equiv.) at ambient temperature. After stirring for 1 h, the mixture was quenched with saturated aqueous NH_4Cl and then extracted with CH_2Cl_2. The combined organic layer was dried over $MgSO_4$ and concentrated in vacuo. The residue was purified by flash column chromatography on silica gel.

*4.1.5.1. 3-(4-Chlorobenzyl)-N-(2,4-dimethoxyphenyl)-N-methyl-1H-pyrazole-5-carboxamide (**43**).*

3-(4-Chlorobenzyl)-1*H*-pyrazole-5-carboxylic acid (**5a**) (86.0 mg, 0.363 mmol) and 2,4-dimethoxy-*N*-methylaniline (60.7 mg, 0.363 mmol) afforded 76.1 mg (54%) of **43** as pale yellow solid. **43** was purified by flash column chromatography on silica gel (EtOAc: *n*-hexane = 1 : 1 to 3 : 1): ^{1}H NMR ($CDCl_3$, 400 MHz) δ 7.18 (d, 2H, J = 8.4 Hz, Ar−H), 7.02 (dd, 1H, J = 7.9, 0.8 Hz, Ar−H), 6.97 (d, 2H, J = 8.3 Hz, Ar−H), 6.43 (s, 1H, Ar−H), 6.41 (d, 1H, J = 2.6 Hz, Ar−H), 4.68 (s, 1H, pyrazole−H), 3.83 (s, 3H, OCH_3), 3.78 (s, 2H, Ar−CH_2), 3.62 (s, 3H, OCH_3), 3.30 (s, 3H, OCH_3); ^{13}C NMR ($CDCl_3$, 100 MHz) δ 161.2, 160.9, 156.4, 151.8, 138.1, 136.9, 131.9, 130.2, 129.8, 128.4, 125.0, 106.1, 104.6, 99.8, 55.7, 55.7, 37.3, 33.8; LR-MS (ESI+) m/z 386 $[M + H]^+$; HR-MS (ESI+) calcd for $C_{20}H_{21}ClN_3O_3$ $[M + H]^+$ 386.1266; found 386.1278.

*4.1.5.2. 3-(4-Chlorobenzyl)-N-(2,4-dimethoxyphenyl)-1-methyl-1H-pyrazole-5-carboxamide (**46**).*

3-(4-Chlorobenzyl)-1-methyl-1*H*-pyrazole-5-carboxylic acid (**45**) (74.7 mg, 0.298 mmol) and 2,4-dimethoxyaniline (42.5 μL, 0.298 mmol) afforded 100 mg (87%) of **46** as ivory solid. **46** was purified by flash column chromatography on silica gel (CH_2Cl_2: EtOAc = 3 : 1 to EtOAc: *n*-hexane = 1 : 1): ^{1}H NMR ($CDCl_3$, 400 MHz) δ 8.21 (m, 1H, Ar−H), 8.02 (s, 1H, NH), 7.27 (d, 2H, J = 8.6 Hz, Ar−H), 7.19 (d, 2H, J = 8.7 Hz, Ar−H), 6.49 (m, 2H, Ar−H), 6.33 (s, 1H, pyrazole−H), 4.17 (s, 3H, CH_3), 3.95 (s, 2H, Ar−CH_2), 3.85 (s, 3H, OCH_3), 3.80 (s, 3H, OCH_3); ^{13}C NMR ($CDCl_3$, 100 MHz) δ 157.5, 157.0, 149.8, 149.6, 138.1, 136.8, 132.3, 130.2, 128.8, 121.0, 120.6, 105.3, 104.0, 98.8, 55.9, 55.7, 39.2, 34.0; LR-MS (ESI+) m/z 386 $[M + H]^+$; HR-MS (ESI+) calcd for $C_{20}H_{21}ClN_3O_3$ $[M + H]^+$ 386.1266; found 386.1283.

*4.1.6. Ethyl 3-(4-chlorobenzyl)-1-methyl-1H-pyrazole-5-carboxylate (**44**).*

To a stirred solution of ethyl 3-(4-chlorobenzyl)-1*H*-pyrazole-5-carboxylate (**4a**) (278 mg, 1.05 mmol) in DMF (3.00 mL) were added K_2CO_3 (218 mg, 1.58 mmol) and iodomethane (98.4 μL, 1.58 mmol) at ambient temperature. After stirring for 10 h, the

reaction mixture was quenched with H_2O and then extracted with EtOAc. The combined organic layer was dried over $MgSO_4$ and concentrated in vacuo. The residue was purified by flash column chromatography on silica gel (EtOAc: *n*-hexane = 1 : 5) to afford 129 mg (44%) of **44** as yellow solid: ^{1}H NMR ($CDCl_3$, 500 MHz) δ 7.26 (d, 2H, J = 8.3 Hz, Ar−H), 7.17 (d, 2H, J = 8.3 Hz, Ar−H), 6.53 (s, 1H, pyrazole−H), 4.30 (q, 2H, J = 7.1 Hz, O$\underline{CH_2}$CH$_3$), 4.13 (s, 3H, CH_3), 3.92 (s, 2H, Ar−CH_2), 1.34 (t, 3H, J = 7.1 Hz, OCH$_2\underline{CH_3}$); ^{13}C NMR ($CDCl_3$, 125 MHz) δ 160.0, 150.1, 138.2, 133.5, 132.3, 130.2, 128.8, 110.1, 61.1, 39.4, 34.0, 14.4; LR-MS (ESI+) *m/z* 279 $[M + H]^+$; HR-MS (ESI+) calcd for $C_{14}H_{16}ClN_2O_2$ $[M + H]^+$ 279.0895; found 279.0893.

*4.1.7. Ethyl 3-(4-chlorobenzoyl)-1H-pyrazole-5-carboxylate (**47**).*
To an ethyl 3-(4-chlorobenzyl)-1*H*-pyrazole-5-carboxylate (**4a**) (641 mg, 2.42 mmol) was added TBHP (5.81 mL of a 5.0 M solution in decane) at ambient temperature. After stirring 22 h at 120 °C, the reaction mixture was quenched with H_2O and then extracted with EtOAc. The combined organic layer was dried over $MgSO_4$ and concentrated in vacuo. The residue was purified by flash column chromatography on silica gel (EtOAc: *n*-hexane = 1 : 4) to afford 645 mg (96%) of **47** as white solid.

*4.1.8. 3-(4-Chlorobenzoyl)-N-(2,4-dimethoxyphenyl)-1H-pyrazole-5-carboxamide (**49**).*
To a stirred solution of 3-(4-chlorobenzoyl)-1*H*-pyrazole-5-carboxylic acid (**48**) (93.7 mg, 0.374 mmol) and 2,4-dimethoxyaniline (58.6 μL, 0.411 mmol) in DMF (2.00 mL) were added EDC·HCl (108 mg), HOBt·H_2O (85.9 mg), DMAP (4.57 mg) and DIPEA (97.7 μL) at ambient temperature. After stirring for 24 h, the reaction mixture was quenched with H_2O and diluted with EtOAc. The organic layer was washed with 1 N HCl and dried over $MgSO_4$. The resulting residue was concentrated in vacuo and purified by flash column chromatography on silica gel (EtOAc: *n*-hexane = 1 : 3 to 1 : 1) to afford 117 mg (81%) of **49** as pale red solid: ^{1}H NMR ($CDCl_3$, 400 MHz) δ 11.91 (brs, 1H, NH), 9.09 (s, 1H, NH), 8.39 (d, 1H, J = 8.2 Hz, Ar−H), 8.02 (d, 2H, J = 7.8 Hz, Ar−H), 7.50 (d, 2H, J = 6.8 Hz, Ar−H), 7.46 (s, 1H, pyrazole−H), 6.53 (m, 2H, Ar−H), 3.88 (s, 3H, OCH_3), 3.81 (s, 3H, OCH_3); ^{13}C NMR ($CDCl_3$, 100 MHz) δ 183.5, 158.2, 156.9, 149.8, 140.5, 134.7, 131.0, 129.3, 121.8, 120.9, 120.8, 114.4, 110.4, 104.0, 98.9, 56.0, 55.7; LR-MS (ESI+) *m/z* 386 $[M + H]^+$; HR-MS (ESI+) calcd for $C_{19}H_{17}ClN_3O_4$ $[M + H]^+$ 386.0902; found 386.0915.

4.2. Cell culture

An insulin secreting pancreatic β-cell line derived from a rat insulinoma, INS cells (Biohermes, Shanghai, China), were cultured in a Roswell Park Memorial Institute (RPMI) 1640 medium (Cellgro, Manassas, VA, USA), supplemented with 2 mM L-glutamine, 0.05 mM 2-mercaptoethanol, 11 mM D-glucose, 1% penicillin/streptomycin (Invitrogen Co., Grand Island, NY, USA), 10% fetal bovine serum (FBS), 10 mM HEPES, and 1 mM sodium pyruvate in a humidified atmosphere at 37 °C containing 5% CO_2.

4.3. Cell viability

The INS-1 cells were seeded in a 96-well plate at a density of 1.5×10^4 cells/mL and incubated for 24 h. The cells were treated with compounds at the concentration of 2.5, 5, 10 μM. After incubation for 24 h, 10% (v/v) Ez-Cytox reagent (Daeil Lab Service Co., Seoul, Korea) was added to each well and incubated for 1 h in the incubator. Subsequently, the absorbance (A value) at 450 nm of each well was measured using a microplate reader (PowerWave XS, Bio-Tek Instruments, Winooski, VT, USA). Percentage of cell viability = (Treatment A value − Blank A value)/(Control A value − Blank A value) × 100%. Culture medium mixed with Ez-Cytox reagent was used as a Blank (background control). The control was the cells treated with 0.5% DMSO, set at 100% cell viability. The experiment was performed in triplicate.

4.4. GSIS assays

The INS-1 cells were seeded in a 12-well plate at a density of 2×10^5 cells/mL and incubated. After incubation for 24 h, each well was washed twice with Krebs-Ringer bicarbonate buffer (KRB, pH 7.4) containing 3.3 mM glucose (basal condition). After starvation in fresh KRB for 2 h, the cells were treated with compounds at the concentration of 2.5, 5, 10 μM. In the assay, gliclazide at the same concentration is used as the positive control. After incubation for 30 min, 3.3 mM glucose as basal or 16.7 mM glucose as stimulant was respectively added to each well and further incubated for additional for 1 h. According to the manufacturer's instructions, GSIS was measured using a rat insulin ELISA kit (Gentaur, Shibayagi Co. Ltd., Gunma, Shibukaw, Japan). Subsequently, the absorbance at 450 nm of each well was measured using a microplate reader (PowerWave XS, Bio-Tek Instruments, Winooski, VT, USA). GSI = stimulatory insulin level/basal insulin level. The experiment was performed in triplicate.

4.5. Western blotting assays

The INS-1 cells were seeded in a 6-well plate at a density of 4.75×10^5 cells/mL and incubated for 24 h. The cells were treated with **26** at the concentration of 2.5, 5, 10 μM. The control was the cells treated with 0.5% DMSO. After incubation for 24 h, the cells were lysed with RIPA buffer (Cell Signaling, Danvers, MA, USA) containing 1 mM phenylmethylsulfonyl fluoride for 20 min at 4 °C. The protein concentration was determined using the Pierce™ BCA protein assay kit (Thermo Scientific, Carlsbad, CA, USA). A 20 μg concentration of protein per lane was separated using 10% sodium dodecyl sulfate polyacrylamide gel, the proteins were transferred onto polyvinylidene difluoride membranes and incubated with primary antibodies against PPARγ, PDX-1, phospho-IRS2 (p-IRS2) (Ser731), IRS-2, phospho-PI3K (p-PI3K), PI3K, phospho-Akt (p-Akt) (Ser473), Akt, and glyceraldehyde 3-phosphate dehydrogenase (GAPDH) at room temperature for 1 h. And proteins were incubated with horseradish peroxidase (HRP)-conjugated anti-rabbit secondary antibodies at room temperature for 1 h. All antibodies were purchased from Cell Signaling (Boston, MA, USA). The proteins were visualized using a chemiluminescence system (FUSION Solo, PEQLAB Biotechnologie GmbH, Erlangen, Germany) after 5 min of incubation with ECL Plus western blotting detection reagents (GE Healthcare, Little Chalfont, UK). The experiment was performed in triplicate and representative data presented.

4.6. Myotube formation, glucose uptake and immunoblotting

C2C12 mouse myoblast cell line was obtained from ATCC and cultured in Dulbecco's modified Eagle's medium (DMEM; Invitrogen, Carlsbad, CA, USA) supplemented with 10% FBS (HyClone Laboratories, Logan, UT, USA) and 1% penicillin/streptomycin (Invitrogen) at 37 °C with 5% CO_2 in air. C2C12 myoblast were cultured in DMEM until 90% of confluence. Cells were differentiated into myotubes with DMEM containing 2% horse serum for 4 days and then incubated for 16 h in DMEM containing 2% BSA and 10% FBS in the absence or presence of compounds. Glucose uptake was determined using a 2-(*N*-(7-nitrobenz-2-oxa-1,3-diazol-4-yl) amino)-2-deoxyglucose (2-NBDG) uptake assay kit according to the

manufacture's protocol (Sigma-Aldrich, St Louis, MO, USA). For Western blotting, antibodies for MG53, IRS-1, PI3K, p-PI3K, Akt, p-Akt, and GAPDH were used.

4.7. Statistical analysis

All analyses were determined using SPSS Statistics ver. 19.0 (SPSS Inc., Chicago, IL, USA). Non-parametric comparisons of samples were conducted by the Kruskal–Wallis test to analyze the results. A value of $p < 0.05$ was considered to be statistically significant.

Declaration of competing interest

The authors declare that they have no known competing financial interests or personal relationships that could have appeared to influence the work reported in this paper.

Acknowledgments

This research was supported by the Basic Science Research Program through the National Research Foundation of Korea (NRF) funded by the Ministry of Education (NRF-2018R1D1A 1B07045101).

Appendix A. Supplementary data

Supplementary data to this article can be found online at https://doi.org/10.1016/j.ejmech.2021.113325.

References

[1] M. Laakso, J. Kuusisto, Insulin resistance and hyperglycaemia in cardiovascular disease development, Nat. Rev. Endocrinol. 10 (2014) 293–302.
[2] H. Kolb, D.L. Eizirik, Resistance to type 2 diabetes mellitus: a matter of hormesis? Nat. Rev. Endocrinol. 8 (2012) 183–192.
[3] S.E. Kahn, M.E. Cooper, S.D. Prato, Pathophysiology and treatment of type 2 diabetes: perspectives on the past, present, and future, Lancet 383 (2014) 1068–1083.
[4] S. Wild, G. Roglic, A. Green, R. Sicree, H. King, Global prevalence of diabetes: estimates for the year 2000 and projections for 2030, Diabetes Care 27 (2004) 1047–1053.
[5] S. Basu, J.S. Yudkin, S. Kehlenbrink, J.I. Davies, S.H. Wild, K.J. Lipska, J.B. Sussman, D. Beran, Estimation of global insulin use for type 2 diabetes, 2018-30: a microsimulation analysis, Lancet Diab. Endocrinol. 7 (2019) 25–33.
[6] Y. Lin, Z. Sun, Current views on type 2 diabetes, J. Endocrinol. 204 (2020) 1–11.
[7] J.S. Skyler, Diabetes mellitus: pathogenesis and treatment strategies, J. Med. Chem. 47 (2004) 4113–4117.
[8] B. Ahrén, Islet G protein-coupled receptors as potential targets for treatment of type 2 diabetes, Nat. Rev. Drug Discov. 8 (2009) 369–385.
[9] G.C. Weir, S. Bonner-Weir, Five stages of evolving β-cell dysfunction during progression to diabetes, Diabetes 53 (2004) S16–S21.
[10] M.L. Mohler, Y. He, Z. Wu, D.J. Hwang, D.D. Miller, Recent and emerging anti-diabetes targets, Med. Res. Rev. 29 (2009) 125–195.
[11] D. Sola, L. Rossi, G.P.C. Schianca, P. Maffioli, M. Bigliocca, R. Mella, F. Corlianò, G.P. Fra, E. Bartoli, G. Derosa, Sulfonylureas and their use in clinical practice, Arch. Med. Sci. 11 (2015) 840–848.
[12] S.J. Persaud, Islet G-protein coupled receptors: therapeutic potential for diabetes, Curr. Opin. Pharmacol. 37 (2017) 24–28.
[13] P. Rai, N. Dwibedi, M. Rowneki, D.A. Helmer, U. Sambamoorthi, Dipeptidyl peptidase-4 inhibitors and joint pain: a retrospective cohort study of older veterans with type 2 diabetes mellitus, Am. Health Drug Benef. 12 (2019) 223–231.
[14] M. Monami, B. Nreu, A. Scatena, B. Cresci, F. Andreozzi, G. Sesti, E. Mannucci, Safety issues with glucagon-like peptide-1 receptor agonists (pancreatitis, pancreatic cancer and cholelithiasis): data from randomized controlled trials, Diabetes Obes. Metabol. 19 (2017) 1233–1241.
[15] D. Abrahami, A. Douros, H. Yin, O.H. Yu, J.-L. Faillie, F. Montastruc, R.W. Platt, N. Bouganim, L. Azoulay, Incretin based drugs and risk of cholangiocarcinoma among patients with type 2 diabetes: population based cohort study, Br. Med. J. 363 (2018) K4880.
[16] J.F. Marcinak, M.S. Munsaka, P.B. Watkins, T. Ohira, N. Smith, Liver safety of fasiglifam (TAK-875) in patients with type 2 diabetes: review of the global clinical trial experience, Drug Saf. 41 (2018) 625–640.
[17] T.M.A. Belete, Recent achievement in the discovery and development of novel targets for the treatment of type-2 diabetes mellitus, J. Exp. Pharmacol. 12 (2020) 1–15.
[18] H.E. Hohmeier, H. Mulder, G. Chen, R. Henkel-Rieger, M. Prentki, C.B. Newgard, Isolation of INS-1–Derived cell lines with robust ATP-sensitive K^+ channel-dependent and -independent glucose-stimulated insulin secretion, Diabetes 49 (2000) 424–430.
[19] M.M. Hann, T.I. Oprea, Pursuing the leadlikeness concept in pharmaceutical research, Curr. Opin. Chem. Biol. 8 (2004) 255–263.
[20] J. Tan, T. Zheng, Y. Yu, K. Xu, TBHP-promoted direct oxidation reaction of benzylic C_{sp3}–H bonds to ketones, RSC Adv. 7 (2017) 15176–15180.
[21] J. Kim, I.K. Shim, D.G. Hwang, Y.N. Lee, M. Kim, H. Kim, S.-W. Kim, S. Lee, S.C. Kim, D.W. Cho, J. Jang, 3D cell printing of islet-laden pancreatic tissue-derived extracellular matrix bioink constructs for enhancing pancreatic functions, J. Mater. Chem. B. 7 (2019) 1773–1781.
[22] X. Huang, G. Liu, J. Guo, Z. Su, The PI3K/AKT pathway in obesity and type 2 diabetes, Int. J. Biol. Sci. 14 (2018) 1483–1496.
[23] A.M. Hennige, D.J. Burks, U. Ozcan, R.N. Kulkarni, J. Ye, S. Park, M. Schubert, T.L. Fisher, M.A. Dow, R. Leshan, M. Zakaria, M. Mossa-Basha, M.F. White, Upregulation of insulin receptor substrate-2 in pancreatic β cells prevents diabetes, J. Clin. Invest. 112 (2003) 1521–1532.
[24] T. Du, L. Yang, X. Xu, X. Shi, X. Xu, J. Lu, J. Lv, X. Huang, J. Chen, H. Wang, J. Ye, L. Hu, X. Shen, Vincamine as a GPR40 agonist improves glucose homeostasis in type 2 diabetic mice, J. Endocrinol. 240 (2019) 195–214.
[25] J. Wang, X. Lv, J. Xu, X. Liu, T. Du, G. Sun, J. Chen, X. Shen, J. Wang, L. Hu, Design, synthesis and biological evaluation of vincamine derivatives as potential pancreatic β-cells protective agents for the treatment of type 2 diabetes mellitus, Eur. J. Med. Chem. 188 (2020) 111976.
[26] J.M. Oliveira, S.A. Rebuffat, R. Gasa, R. Gomis, Targeting type 2 diabetes: lessons from a knockout model of insulin receptor substrate 2, Can. J. Physiol. Pharmacol. 92 (2014) 613–620.
[27] S.S. Andrali, M.L. Sampley, N.L. Vanderford, S. Özcan, Glucose regulation of insulin gene expression in pancreatic β-cells, Biochem. J. 415 (2008) 1–10.
[28] J.A. Moibi, D. Gupta, T.L. Jetton, M. Peshavaria, R. Desai, J.L. Leahy, Peroxisome proliferator–activated receptor-γ regulates expression of PDX-1 and NKX6.1 in INS-1 cells, Diabetes 56 (2007) 88–95.
[29] H. Watanabe, H. Saito, H. Nishimura, J. Ueda, B.M. Evers, Activation of phosphatidylinositol-3 kinase regulates pancreatic duodenal homeobox-1 in duct cells during pancreatic regeneration, Pancreas 36 (2008) 153–159.
[30] K.-M. Lee, J.-H. Kim, E.-S. Choi, E. Kim, S.-K. Choi, W.B. Jeon, RGD-containing elastin-like polypeptide improves islet transplantation outcomes in diabetic mice, Acta Biomater. 94 (2019) 351–360.
[31] D. Lee, B.S. Hwang, P. Choi, T. Kim, Y. Kim, B.G. Song, N. Yamabe, G.S. Hwang, K.S. Kang, J. Ham, Hypoxylonol F isolated from *Annulohypoxylon annulatum* improves insulin secretion by regulating pancreatic β-cell metabolism, Biomolecules 9 (2019) 335.
[32] L.H. Cazarolli, P. Folador, H.H. Moresco, I.M.C. Brighente, M.G. Pizzolatti, F.R.M.B. Silva, Stimulatory effect of apigenin-6-C-β-L-fucopyranoside on insulin secretion and glycogen synthesis, Eur. J. Med. Chem. 44 (2009) 4668–4673.
[33] R.G. Damazio, A.P. Zanatta, L.H. Cazarolli, L.D. Chiaradia, A. Mascarello, R.J. Nunes, R.A. Yunes, F.R.M.B. Silva, Antihyperglycemic activity of naphthylchalcones, Eur. J. Med. Chem. 45 (2010) 1332–1337.
[34] L. Pasternak, E. Meltzer-Mats, G. Babai-Shani, G. Cohen, O. Viskind, J. Eckel, E. Cerasi, S. Sasson, A. Gruzman, Benzothiazole derivatives augment glucose uptake in skeletal muscle cells and stimulate insulin secretion from pancreatic β-cells *via* AMPK activation, Chem. Commun 50 (2014) 11222–11225.
[35] A. Mascarello, M.J.S. Frederico, A.J.G. Castro, C.P. Mendes, M.F. Dutra, V.M. Woehl, R.A. Yunes, F.R.M.B. Silva, R.J. Nunes, Novel sulfonyl(thio)urea derivatives act efficiently both as insulin secretagogues and as insulinomimetic compounds, Eur. J. Med. Chem. 86 (2014) 491–501.
[36] N. Rozentul, Y. Avrahami, M. Shubely, L. Levy, A. Munder, G. Cohen, E. Cerasi, S. Sasson, A. Gruzman, A novel phenylchromane derivative increases the rate of glucose uptake in L6 myotubes and augments insulin secretion from pancreatic beta-cells by activating AMPK, Pharm. Res. (N. Y.) 34 (2017) 2873–2890.
[37] L. Xu, M. Xing, X. Xu, F.S.A. Saadeldeen, Z. Liu, J. Wei, W. Kang, Alizarin increase glucose uptake through PI3K/Akt signaling and improve alloxan-induced diabetic mice, Future Med. Chem. 11 (2019) 395–406.
[38] A.C.P. Thirone, C. Huang, A. Klip, Tissue-specific roles of IRS proteins in insulin signaling and glucose transport, Trends Endocrinol. Metabol. 17 (2006) 72–78.
[39] R. Song, W. Peng, Y. Zhang, F. Lv, H.-K. Wu, J. Guo, Y. Cao, Y. Pi, X. Zhang, L. Jin, M. Zhang, P. Jiang, F. Liu, S. Meng, X. Zhang, P. Jiang, C.-M. Cao, R.-P. Xiao, Central role of E3 ubiquitin ligase MG53 in insulin resistance and metabolic disorders, Nature 494 (2013) 375–379.
[40] J.S. Park, H. Lee, B.W. Choi, S. Ro, D. Lee, J.E. Na, J.-H. Hong, J.-S. Lee, B.-W. Kim, Y.-G. Ko, An MG53-IRS1-interaction disruptor ameliorates insulin resistance, Exp. Mol. Med. 50 (2018) 1–12.